The Journal of Immunology

Ca^{2+}–Calcineurin Axis–Controlled NFAT Nuclear Translocation Is Crucial for Optimal T Cell Immunity in an Early Vertebrate

Xiumei Wei, Huiying Li, Yu Zhang, Cheng Li, Kang Li, Kete Ai and Jialong Yang

J Immunol 2020; 204:569-585; Prepublished online 23 December 2019;
doi: 10.4049/jimmunol.1901065
http://www.jimmunol.org/content/204/3/569

The Journal of Immunology is published twice each month by
The American Association of Immunologists, Inc.,
1451 Rockville Pike, Suite 650, Rockville, MD 20852

Print ISSN: 0022-1767 Online ISSN: 1550-6606.

Ca^{2+}–Calcineurin Axis–Controlled NFAT Nuclear Translocation Is Crucial for Optimal T Cell Immunity in an Early Vertebrate

Xiumei Wei,*,[1] Huiying Li,*,[1] Yu Zhang,* Cheng Li,* Kang Li,* Kete Ai,* and Jialong Yang*,†

Calcium ion (Ca^{2+}) is a widespread and primitive second messenger that regulates physiological cell functions in almost all life beings. Ca^{2+} influx-induced NFAT activation is essential for T cell function and adaptive immunity. However, whether and how Ca^{2+} signaling modulates T cell immunity in early vertebrates, especially in nontetrapods, remains largely unknown. To address these questions, a Nile tilapia (*Oreochromis niloticus*) model was employed to investigate the regulation of ancestral T cell immunity by Ca^{2+}–NFAT signaling in jawed fish. In Nile tilapia, an evolutionarily conserved Ca^{2+}–NFAT signaling pathway is involved in the primary adaptive immune response during *Streptococcus agalactiae* infection. Meanwhile, T cell signals trigger several events along the Ca^{2+}–NFAT axis in this early vertebrate, including Ca^{2+} influx, calcineurin activation, and NFAT nuclear import. More critically, suppression of Ca^{2+}–NFAT signaling by the calcineurin inhibitor cyclosporine A impairs primordial T cell activation, clonal expansion, and infection clearance. Mechanistically, Nile tilapia NFAT interacts with several other transcription factors for potent gene expression, and T cells in this nontetrapod employ Cabin1 and DYRK1A to regulate NFAT nuclear import and export, respectively. To the best of our knowledge, this study is the first to demonstrate the regulatory mechanism of Ca^{2+}–NFAT signaling on T cell immunity in a nontetrapod species. We suggest that modulation of T cell immunity by Ca^{2+}–NFAT signaling is a primitive strategy that already existed prior to the divergence of bony fish from the tetrapod lineage. The findings of this study provide valuable perspectives for understanding the evolution of adaptive immune system.
***The Journal of Immunology*, 2020, 204: 569–585.**

During evolution, cells have adopted positively charged calcium ion (Ca^{2+}) and negatively charged phosphate ions as two universal tools for signal transduction (1). Benefiting from the rapid switch between on and off statuses, strong homeostasis via influx/efflux, and the ability to interact with thousands of proteins (2), Ca^{2+} acts as a versatile second messenger and plays pivotal roles in nearly every cellular process, including excitability, motility, metabolism, exocytosis, apoptosis, transcription, and immunity (1, 2). To achieve this versatility, cells employ a number of components to assemble a Ca^{2+} signaling system with wide spatial and temporal dynamics (2). Among these components, the Ca^{2+} release–activated calcium (CRAC) channel, which mediates intracellular Ca^{2+} increase, and its tightly regulated NFAT are of paramount importance for T cell immunity (3–5).

Engagement of the TCR triggers the activation of protein tyrosine kinases, such as LCK and ZAP70, and eventually results in tyrosine phosphorylation of phospholipase Cγ1 (PLCγ1). Activated PLCγ1 further hydrolyzes the membrane phospholipid phophatidylinositol-4,5-biphosphate (PIP2) and generates two second messengers inositol 1,4,5-triphosphate (IP_3) and diacylglycerol (DAG) (6, 7). DAG triggers the MAPK/ERK and PKCθ-IKK-NF-κB pathways, whereas IP_3 binds to the IP_3 receptor (IP_3R) on the endoplasmic reticulum (ER) membrane to permit Ca^{2+} efflux from ER Ca^{2+} stores into the cytoplasm (7). Depletion of ER Ca^{2+} activates CRAC channel in the plasma membrane and induces sustained Ca^{2+} influx from extracellular compartment into the cytoplasm, which is required for optimal TCR-induced signal transduction (8, 9). An increase in intracellular Ca^{2+} is sensed by the EF hands of calcium-binding protein calmodulin, which in turn activates phosphatase activity of the serine/threonine phosphatase calcineurin. Activated calcineurin dephosphorylates cytoplasmic NFAT, which exposes its nuclear localization sequence and leads to rapid nuclear import (10). In the nuclear, NFAT cooperates with multiple transcription factors from other signaling pathways, such as AP-1 and NF-κB, to induce transcription of specific genes that control T cell activation, proliferation, and differentiation (10–13).

NFAT-driven gene expression and T cell immunity are highly dependent on sustained Ca^{2+} influx and calcineurin activity. For

*State Key Laboratory of Estuarine and Coastal Research, School of Life Sciences, East China Normal University, Shanghai 200241, China; and †Laboratory for Marine Biology and Biotechnology, Qingdao National Laboratory for Marine Science and Technology, Qingdao 266071, China

[1]X.W. and H.L. contributed equally to this work.

ORCID: 0000-0002-3112-5012 (J.Y.).

Received for publication August 30, 2019. Accepted for publication November 22, 2019.

This work was supported by the National Natural Science Foundation of China (31972822 and 31872591), the Shanghai Pujiang Program (18PJ1402700), and the Fundamental Research Funds for the Central Universities.

Address correspondence and reprint requests to Prof. Jialong Yang, East China Normal University, 500 Dongchuan Road, Shanghai 200241, China. E-mail address: jlyang@bio.ecnu.edu.cn

The online version of this article contains supplemental material.

Abbreviations used in this article: Cabin1, calcineurin-binding protein 1; CRAC, Ca^{2+} release–activated calcium; DYRK1A, dual-specificity tyrosine phosphorylation-regulated kinase 1A; ECNU, East China Normal University; ER, endoplasmic reticulum; GSK3, glycogen synthase kinase 3; IP_3, inositol 1,4,5-triphosphate; IP_3R, IP_3 receptor; NCBI, National Center for Biotechnology Information; NJ, neighbor-joining; PLCγ1, phospholipase Cγ1; qPCR, quantitative real-time RT-PCR; RHD, Rel homology domain; siRNA, small interfering RNA; Treg, regulatory T.

example, inhibition of CRAC channel impairs TCR-induced Ca^{2+} signaling, T cell activation, and proliferation (8, 14). In addition, deficiency of STIM1 or ORAI1, two key regulators of CRAC channel, dramatically impairs cytokine production in T cells, including IL-2, IL-4, IL-17, TNF, and IFN-γ, and thus increases susceptibility to pathogen infection (4, 5, 15–19). Calcineurin is the only phosphatase that promotes NFAT nuclear import, its activity is regulated by not only upstream Ca^{2+} and calmodulin but also by multiple endogenous calcineurin inhibitors (10, 20, 21). For example, calcineurin-binding protein 1 (Cabin1) interacts with calcineurin to block its activity, inhibiting NFAT dephosphorylation and nuclear translocation (22, 23). Additionally, A-kinase anchor protein 79 (AKAP79) prevents calcineurin from accessing to NFAT substrates by tethering calcineurin to the membrane (24, 25), and members of the calcipressin family constitute additional calcineurin regulators (26). In the absence of these molecules, mouse T cells exhibit a lower threshold for T cell stimulation and increased production of cytokines in response to TCR ligation (10, 20, 26, 27), emphasizing the important roles of these calcineurin inhibitors in T cell immunity. Moreover, when intracellular Ca^{2+} concentration decreases, nuclear NFAT is immediately rephosphorylated and inactivated via the coordinated action of multiple NFAT kinases, such as glycogen synthase kinase 3 (GSK3) and casein kinase 1 (CK1), and this inactivation results in relocation of NFAT to the cytoplasm (28, 29). Recent studies have also identified dual-specificity tyrosine phosphorylation-regulated kinase 1A (DYRK1A) as a physiological negative regulator of NFAT-driven gene transcription that enables the phosphorylation of NFAT by CK1 and GSK3 in the nucleus (30, 31).

Although Ca^{2+} signaling is an ancient and evolutionarily conserved pathway that exists in almost all animals (32), studies on the regulatory mechanism of this signaling pathway in T cell immunity have mainly been restricted to mammalian models, and whether and how Ca^{2+}–NFAT signaling modulates T cell immune response in early vertebrates remains to be elucidated. As fish species are the earliest evolutionary group to possess T cells, uncovering the immune function and related mechanisms in these ancestral T cells will undoubtedly provide valuable evidence for understand the evolution of T cell immunity. Recent advances have identified several suspected T cell populations, such as $CD3^+$, $CD4\text{-}1^+$, $CD4\text{-}2^+$, $CD8\alpha^+$, or $TCR\gamma\delta^+$ leukocytes, in a variety of teleost species (33–36). Like mammalian $CD8^+$ T cells, primitive $CD8^+$ leukocytes in bony fish express high levels of perforin A, granzyme B, and IFN-γ in response to pathogen infection and mediate protection against secondary infection (33, 36–38), suggesting that these cells have potential cytotoxic and memory properties in the context of cellular immunity. The $CD4^+$ leukocyte subpopulation has been reported to have the capacity to differentiate into Th2-like and regulatory T (Treg)-like cells in teleost (39–41). Furthermore, Th2-specific genes are markedly induced by IL-4 in zebrafish, and interaction of IL-4 with its receptor promotes CD40 expression on B cells and enhances the costimulatory response (41). Treg-like cells mediate organ-specific regenerative programs in zebrafish (40), and depletion of $CD4^+CD25^+Foxp3^+$ Treg-like cells in puffer fish produces an enhanced lymphocyte reaction and augments intestinal inflammation (39). Thus, the T cell response appears to be a universal feature of adaptive immunity among jawed vertebrates.

Although equivalent T cell populations with similar immunological functions have emerged in bony fish, the underlying regulatory mechanisms of immune response mediated by these primordial T cells are still largely unknown. In our previous study, we used a Nile tilapia (*Oreochromis niloticus*) model to show that mTORC1 signaling is indispensable for teleost T cell activation, proliferation, and effector function and that mTORC1 directs T cell function by regulating metabolic reprogramming (42); these findings indicate that primordial T cells are armed with sophisticated regulatory strategies similar to those reported in modern T cells. In the current study, we identified an evolutionarily conserved Ca^{2+}–NFAT signaling pathway in Nile tilapia and found that T cell signals induce several hallmarks of Ca^{2+}–NFAT activation in this early vertebrate, including IP_3R phosphorylation, Ca^{2+} influx, calcineurin activation, and NFAT nuclear import. In addition, inhibition of calcineurin activity by cyclosporine A impaired teleost T cell activation, proliferation, and infection clearance. Furthermore, NFAT-driven activation of primitive T cells was found to be negatively regulated by cytosolic Cabin1 and nuclear DYRK1A, which serve as a calcineurin inhibitor and an NFAT kinase, respectively. To the best of our knowledge, this study is the first to demonstrate the mechanism by which Ca^{2+}–NFAT signaling regulates the adaptive immune system in a fish species. Our data suggest that modulation of T cell immunity by Ca^{2+}–NFAT signaling might be an ancestral trait that already existed by the appearance of adaptive immunity 450 million years ago, and the results therefore provide valuable insight into the evolutionary history of T cell subset.

Materials and Methods

Ethics statement

All experiments were conducted in accordance with the Guide for the Care and Use of Laboratory Animals of the Ministry of Science and Technology of China. The experimental procedures were approved by the East China Normal University (ECNU) Experimental Animal Ethics Committee. All efforts were made to minimize the suffering of experimental animals.

Fish maintenance

Nile tilapia larvae with a body length of 3–4 cm were purchased from an aquatic farm in Guangzhou, Guangdong Province, China. All the fish were maintained in fresh water at 28°C with continuous aeration and fed daily with commercial pellets. When the body length reached 8–10 cm, healthy fish, as determined by general appearance and activity, were used for the study.

Sequence, structure, and phylogenetic analysis

The cDNA and amino acid sequences of related genes in Nile tilapia were obtained from the whole-genome sequence with the assembly identifier GCA_001858045.3 in National Center for Biotechnology Information (NCBI) GenBank (https://www.ncbi.nlm.nih.gov/genome/annotation_euk/Oreochromis_niloticus/104/) (43). Sequences of Nile tilapia Ca^{2+}–NFAT components in the NCBI GenBank were mined by searching the protein name of their mammalian homologs. The sequences of other species were obtained from NCBI GenBank (https://www.ncbi.nlm.nih.gov) or Ensemble (http://asia.ensembl.org/index.html). The accession numbers of these genes are listed in Supplemental Tables I and II. Amino acid sequences were analyzed by BLAST, protein domains were predicted with SMART version 4.0, and sketch maps of domain organization were prepared with DOG version 2.0 software. Based on homology analysis, multiple sequence alignment was carried out using ClustalW. Tertiary structures of proteins were predicted by the SWISS-MODEL server, and the results were displayed in PyMOL version 0.97. Phylogenetic trees were constructed using MEGA4.1 software with the neighbor-joining (NJ) algorithm.

Streptococcus agalactiae *infection*

S. agalactiae was cultured in Brain Heart Infusion broth to the exponential growth phase, and cells were collected and resuspended in PBS to a concentration of 7×10^7 CFU for infection. Nile tilapia were injected i.p. with 100 μl *S. agalactiae* suspension as the infection group; the same volume of PBS was injected in the control group. The two groups of fish were maintained at 28°C with aeration and fed daily.

Leukocyte isolation

Peripheral blood was collected from caudal vessels, mixed immediately with prechilled anticoagulant (8.17 g/l NaCl, 5.46 g/l citric acid, 8.82 g/l

sodium citrate, 19.8 g/l glucose, 3.72 g/l EDTA [pH 6.6]), centrifuged, and resuspended in FBS-free DMEM. The spleen and head kidney were harvested, smashed in DMEM, and collected through nylon mesh. The leukocytes were isolated according to previous report (42). In brief, 100% Percoll, which was prepared by mixing Percoll solution (GE Healthcare) with 10× PBS at a ratio of 9:1, was diluted into 51 or 34% with DMEM (v/v). Then, 4 ml of 51% and 4 ml of 34% Percoll were slowly added into a 15 ml tube to obtain a discontinuous layer, and cell suspensions of the blood, spleen, or head kidney samples were layered onto the 51/34% discontinuous Percoll density gradient. After centrifugation at 500 × *g* for 30 min with the lowest acceleration and deceleration, the cells accumulated at the interface were collected, washed twice and resuspended in DMEM (10% FBS) for further experiments.

Leukocyte stimulation

For T cell activation and proliferation, spleen leukocytes were cultured in DMEM (10% FBS) containing 1 μg/ml PHA for different times, after which the cells were harvested for quantitative real-time RT-PCR (qPCR) analysis or flow cytometry. For immunoblotting analysis, after resting in DPBS for 30 min, spleen leukocytes were stimulated with 50 ng/ml PMA plus 500 ng/ml ionomycin for different times and then lysed in RIPA lysis buffer (50 mM Tris, 150 mM NaCl, 1% Triton X-100, 1% sodium deoxycholate, 0.1% SDS) with freshly added protease inhibitor (1:1000; Sigma-Aldrich) and phosphorylase inhibitor (1:100; Sigma-Aldrich). The stimulated cells were also harvested for immunofluorescence analysis, Ca^{2+} influx, or calcineurin activity examination.

Ca^{2+} influx assay

A 10^7 sample of spleen leukocytes in 1 ml loading buffer (1% FBS and 10 mM HEPES in HBSS without phenol red) were incubated with 2.5 μg/ml Indo-1 (Life Technologies) in the presence of Pluronic at 30˚C for 30 min. After washing with loading buffer, the cells were collected on a BD Biosciences flow cytometer to obtain the baseline fluorescence of the 450:510 nm ratio on the lymphocyte population. Then, 1 μg/ml PHA or 2 μg/ml of thapsigargin was added to induce Ca^{2+} influx. Cells from three Nile tilapia individuals were prepared, stimulated, and analyzed, respectively. The ratios of 450:510 nm, for both baseline and after stimulation, were used for statistics.

Small interfering RNA interference

Three pairs of small interfering RNAs (siRNAs) targeting Nile tilapia Cabin1 synthesized by GenePharma (Shanghai, China) were dissolved to 20 μM and mixed with an equivalent amount of Lipo6000 transfection reagent (1:5 diluted with PBS; Beyotime) as the working solution. Nile tilapia individuals were i.p. injected with 100 μl working solution to knockdown Cabin1. Nonspecific siRNA synthesized by the same company was used as a negative control. Two days after injection, the spleen or spleen leukocytes were collected for further qPCR, Western blot, and enzyme activity assays. The sequences of the Cabin1 siRNA and control siRNA are listed in Supplemental Table II.

qPCR

Spleen leukocytes that were or were not subjected to stimulation/infection/treatment were resuspended in TRIzol reagent (Invitrogen) for total RNA extraction according to the manufacturer's instructions. After digestion with DNase I (Promega) at 37˚C for 30 min, the cDNA was synthesized with a First Strand cDNA Synthesis Kit (Thermo Fisher Scientific) using total RNA as the template and oligo (dT)-adapter as the primer. qPCR was performed with SYBR Green Mix (Takara) on a Connect Real-Time System (Bio-Rad). The qPCR program was set as follows: 180 s at 95˚C as initial denaturation, followed by 40 cycles of 10 s at 95˚C for denaturation plus 30 s at 59˚C as annealing. Dissociation curve of amplification products was performed at the end of each PCR to confirm that only one product was amplified. β-Actin was selected as the internal control. All specific primers are listed in Supplemental Table II. The relative gene expression level was analyzed by the $2^{-\triangle\triangle \text{cycle threshold}}$ method.

Immunofluorescence assay

A total of 1×10^6 spleen leukocytes were rested in DPBS for 30 min before the cells were stimulated with 50 ng/ml PMA plus 500 ng/ml ionomycin. The stimulation was stopped by adding 500 μl precooled PBS, and the cells were then centrifuged onto slides using Cytospin 4. The cells were fixed with prechilled acetone for 15 min, and then with 0.5% Triton X-100 for another 15 min. After blocking with 3% BSA in PBS at room temperature for 1 h, the cells were stained with 1:100 diluted rabbit–anti phospho-IP_3R (8548; Cell Signaling Technology), rabbit-anti calmodulin (4830; Cell Signaling Technology) or mouse-anti NFAT1 (sc-7296; Santa Cruz Biotechnology) as primary Abs at room temperature for 1 h. After three washes with PBS, the cells were incubated with Alexa Fluor 488–conjugated goat–anti-mouse IgG (Abcam) or Alexa Fluor 594–conjugated goat–anti-rabbit IgG (Abcam) as secondary Abs for 1 h. After washing and mounting with mounting solution containing DAPI, the cells were observed using a Zeiss ApoTome Microscope and analyzed with Photoshop CS4 software. Three groups of slides prepared from three Nile tilapia individuals were observed for statistic. To calculate the percentage of phospho-IP_3R or calmodulin-positive cells, the number of positive events within 100 cells under several random views were counted in each slide. For NFAT1, 100 NFAT1-positive cells under several random views were first recorded in each slide, and the number of the cells with positive signal in the nucleus was recorded for statistic.

Specific inhibitor treatment

Nile tilapia individuals were i.p. injected with 100 μl cyclosporine A (MedChemExpress) at a dosage of 15 mg/kg/d on the indicated days to suppress calcineurin activity, and leukocytes were isolated for assay. When in vitro culture was performed, 1 nM of cyclosporine A was added to continuously inhibit the calcineurin. To calculate the survival percentage, fish infected with *S. agalactiae* were i.p. injected with cyclosporine A, and the number of dead individuals was recorded daily. To inhibit DYRK1A, Nile tilapia individuals were i.p. injected with 100 μl of the inhibitor harmine (MedChemExpress) at a dosage of 10 mg/kg/d for two consecutive days. Spleen leukocytes were then isolated and stimulated with PHA or PMA plus ionomycin in vitro as described above for assay.

Calcineurin enzyme activity

Spleen leukocytes from cyclosporine A–treated or untreated Nile tilapia were stimulated with 1 μg/ml PHA or 50 ng/ml PMA plus 500 ng/ml ionomycin for different times. The cells were homogenized in normal saline on ice for 2 min and centrifuged at 10,000 rpm at 4˚C for 10 min. The supernatant was used to examine the enzyme activity and protein concentration. The protein concentration was measured with a BCA Protein Assay Kit (Beyotime). Calcineurin activity was assessed with a calcineurin assay kit (Nanjing Jiancheng Bioengineering Institute, Nanjing, China) according to the manufacturer's instructions, and calculated as per mg protein. Calcineurin activity in spleen leukocytes from control siRNA– and Cabin1 siRNA–injected Nile tilapia was also examined as above 2 d after siRNA injection.

In vitro proliferation

Spleen leukocytes from Nile tilapia treated or not treated with cyclosporine A for two consecutive days were isolated and labeled with 10 μM CFSE (Invitrogen) at room temperature for 9 min according to the manufacturer's instructions. After washing twice with DMEM, the cells were cultured in DMEM (10% FBS) containing 1 μg/ml PHA in the presence or absence of 1 nM of additional cyclosporine A for 48 h. The proliferation of lymphocytes was detected by flow cytometry; 7AAD (1:400; Life Technologies) was added to the samples shortly before collection to identify live/dead cells.

Flow cytometry

Freshly isolated or CFSE-labeled leukocytes were resuspended in PBS containing 2% FBS for FACS analysis. For intracellular LCK staining, spleen leukocytes were fixed with Cytofix/Cytoperm buffer (BD Biosciences) on ice for 30 min and washed twice with Perm/Wash solution (BD Biosciences). After staining with an Alexa Fluor 647–conjugated-LCK Ab (LCK-01; BioLegend) on ice for 30 min, the cells were washed twice with Perm/Wash solution and resuspended in the same solution. All samples were evaluated using a BD Biosciences FACSCalibur flow cytometer. Data were analyzed using FlowJo software.

Plasmid construction, transfection, and coimmunoprecipitation assay

Full-length fragments of transcription factors with different tags, including NFAT1-Flag, NFAT1-HA, c-Fos-HA, NIP45-HA, T-bet-HA, IRF4-HA, EGR1-HA, and Foxp3-HA, were amplified from Nile tilapia cDNA with corresponding primers (Supplemental Table II). After digestion with restriction enzymes, these fragments were ligated into pEGFP-C1 to construct transfection vectors. HEK 293T cells seeded in 6-cm^2 dishes overnight were cotransfected with 5 μg NFAT1-Flag-pEGFP-C1 plasmid and 5 μg partner-HA-pEGFP-C1 plasmid, as indicated in the figures.

At 48 h posttransfection, the cells were harvested and lysed in RIPA lysis buffer with freshly added protease inhibitors. The supernatants obtained were used for coimmunoprecipitation assay, which was performed using anti-Flag Ab-conjugated agarose beads (Sigma-Aldrich). Briefly, 10 μl anti-Flag Ab-conjugated agarose beads were added to the lysate of transfected 293T cells and incubated at 4˚C overnight with shaking. After washing four times with lysis buffer, the beads were suspended in SDS loading buffer and denatured at 95˚C for 10 min, followed by Western blot assay.

Western blot analysis

Homogenized Nile tilapia tissues or spleen leukocytes were lysed in RIPA lysis buffer as described above, and nuclear proteins were extracted using a Nuclear Protein Extracting Kit (Beyotime) according to the manufacturer's instructions. For Western blot analysis, the samples were separated by 12% SDS-PAGE with a steady current of 40 mA, and then the protein was transferred to nitrocellulose membrane at 100 V for 2 h. After blocking with 4% skim milk powder in phosphate-buffered saline with 0.05% tween (PBST) at room temperature for 1 h, the blots were incubated with 1:1000 diluted primary Abs against calmodulin (4830), calcineurin (2614), IP_3R (8568), phospho-IP_3R (8548), phospho-GSK3β (9323), Histone H3 (9717), β-actin (4970), TBP (44059) from Cell Signaling Technology, 1:1000 diluted NFAT1 Ab (sc-7296; Santa Cruz Biotechnology), 1:2000 diluted Flag or HA Abs (Sigma-Aldrich) at 4˚C overnight. The blots were washed three times with phosphate-buffered saline with 0.05% tween (PBST) and then further incubated with 1:10,000 diluted goat–anti rabbit or mouse IgG H and L chain–conjugated with Alexa Fluor 790 or 680 (Abcam) as the secondary Ab at room temperature for 1 h. Another three times of washes were performed before the blotting results were acquired using Odyssey CLx Image Studio. β-Actin and histone H3 or TBP were selected as internal controls for total and nuclear proteins, respectively.

Statistical analysis

All data are presented as the mean ± SEM. Statistical evaluations of differences were conducted by a two-tailed Student *t* test; *p* values were as follows: $*p < 0.05$, $**p < 0.01$, and $***p < 0.001$.

Results

An evolutionarily conserved Ca^{2+}–NFAT axis is present in Nile tilapia

To begin our study, an indepth search for Ca^{2+}–NFAT signaling components was performed in the Nile tilapia genome sequence available in NCBI GenBank. All components of the classical Ca^{2+}–NFAT pathway, including IP_3R, calmodulin, calcineurin-A, NFAT1, NFAT2, and NFAT4, were identified in Nile tilapia (Fig. 1A, Supplemental Table I), indicating the potential presence of Ca^{2+}–NFAT pathway in this early vertebrate. As an initial receptor that senses the intracellular second messenger IP_3, Nile tilapia IP_3R shares a domain organization similar to that of the mouse receptor (Fig. 1B). Both proteins consist of four tandem MIR domains that function as ligand transferases and two tandem RYDR-ITPR domains that contain IP_3 binding sites, followed by an RIH-assoc domain and an Ion-trans domain with six transmembrane helices (Fig. 1B). Downstream of IP_3R, Nile tilapia calmodulin also exhibits a pattern similar to that of its homolog from mouse in the arrangement of its four functional EF-hand domains, which have potential calcium-binding function (Fig. 1C). The same is true for calcineurin-A, with both Nile tilapia and mouse calcineurin-A comprising a catalytic domain, a calcineurin-B-binding motif, and a calmodulin-binding motif (Fig. 1D). Similarly, the functional domains or motifs of NFAT1, NFAT2, and NFAT4, including the calcineurin-binding motif, nuclear localization signal, nuclear export signal, and Rel homology domain (RHD), also adopt similar organizations in Nile tilapia and mouse (Fig. 1E). However, one exception is that Nile tilapia NFAT2 has a longer C terminus than does its counterpart from mouse (Fig. 1E).

Moreover, primary and tertiary structures of Nile tilapia calmodulin and calcineurin-A, which are associated with Ca^{2+} binding and signaling transduction, are well conserved with those of homologs from other species (Fig. 1F, 1G, Supplemental Fig. 1A). Notably, the amino acid sequences of calmodulin from seven selected vertebrates are entirely the same (Fig. 1F), suggesting high conservation of this molecule during evolution. In addition, amino acid sequences of Nile tilapia NFATs, especially the RHD, which is responsible for the DNA binding that is usually found in a family of eukaryotic transcription factors, also show high conservation with the counterparts in other vertebrates (Supplemental Fig. 1B). Moreover, phylogenetic trees show that Nile tilapia IP_3R, calcineurin-A, NFAT1, NFAT2, and NFAT4 cluster with their homologs from other teleost (Fig. 1H, 1I, Supplemental Fig. 2). Taken together, these results suggest that the teleost Nile tilapia encodes an intact and conserved Ca^{2+}–NFAT pathway, which might perform functions similar to those reported in higher vertebrates.

Nile tilapia Ca^{2+}–NFAT axis participates in the primary adaptive immune response

Because a potential Ca^{2+}–FAT pathway was found in Nile tilapia, we sought to determine in which tissue this signaling pathway functions. Western blot assays using specific Abs revealed that the Nile tilapia calmodulin protein is highly expressed in the gill, intestine, spleen, liver, and head kidney and is relatively lower in the skin, trunk kidneys, and muscle (Fig. 2A, 2B). The expression level of calcineurin is relatively higher in gill and spleen, intermediate in skin, liver, head kidney, trunk kidney, and muscle, and lower in intestine (Fig. 2A, 2C). These results suggest that Ca^{2+}–NFAT might be a constitutive signaling pathway with a broad tissue distribution in Nile tilapia.

To determine whether the Ca^{2+}–NFAT pathway is involved in the adaptive immune response, we infected Nile tilapia with the pathogen *S. agalactiae* using a sublethal dose that caused an ∼30% death rate within 10 d according to our previous study (42), and the expression level of Ca^{2+}–NFAT components in spleen lymphocytes was examined by qPCR and Western blot in the primary response stage. Transcripts of IP_3R, calmodulin, and calcineurin-A were significantly induced at 3, 5, or 8 d postinfection (Fig. 2D). Similarly, compared with their counterparts, the protein levels of calmodulin and calcineurin were also increased in spleen lymphocytes of *S. agalactiae*–infected fish at 3 or 5 d postinfection (Fig. 2E, 2F). Although mRNA expression of NFAT1 was comparable between infected and control animals (Fig. 2G), NFAT1 protein was obviously elevated during bacterial infection (Fig. 2E, 2F). In addition, mRNA level of NFAT2, but not NFAT4, was dramatically increased in response to pathogen infection (Fig. 2G). Although we could not assess the protein expression patterns of NFAT2 and NFAT4 during bacterial infection because of the lack of effective Abs, our results indicate that Ca^{2+}–NFAT pathway participates in the primary response of lymphocyte-mediated adaptive immunity in Nile tilapia.

T cell signals induce sustained Ca^{2+} influx and calcineurin activation in Nile tilapia

Next, we examined how Ca^{2+}–NFAT signaling participates in lymphocyte-mediated adaptive immunity in Nile tilapia. The T cell–specific mitogen PHA was used to stimulate Nile tilapia spleen lymphocytes in vitro. Upon T cell activation, IP_3R mRNA or protein expression was not upregulated (Fig. 3A, 3B). However, further investigation revealed that phosphorylation of IP_3R, which is crucial for Ca^{2+} release, was dramatically increased in spleen lymphocytes following activation by PMA and ionomycin (Fig. 3B). Enhancement of IP_3R phosphorylation was also confirmed by confocal microscopy (Fig. 3C), suggesting that IP_3R mainly participates in Nile tilapia lymphocyte activation via

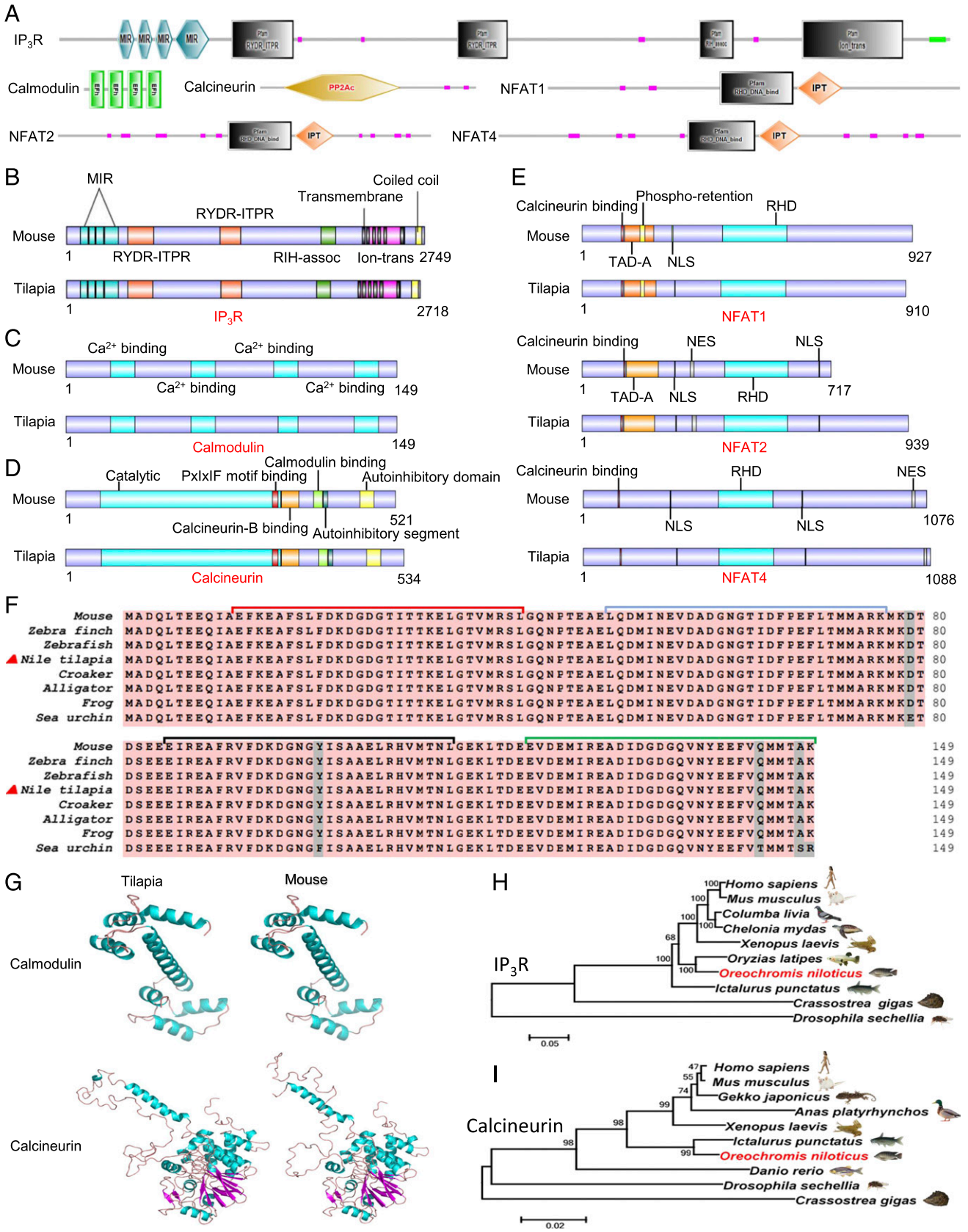

FIGURE 1. Evolutionary conservation of Nile tilapia Ca^{2+}–NFAT signaling components. (**A**) Domain prediction of Nile tilapia Ca^{2+}–NFAT components by the SMART program. (**B**–**E**) Comparison of the domain organization of IP_3R (B), calmodulin (C), calcineurin-A (D), and NFAT (E) proteins from the indicated species. (**F**) Multisequence alignment analysis of calmodulin from Nile tilapia with homologs from other animals. Amino acids with 100% identity are in red, and similar amino acids are in gray. The four EF-hand domains are labeled. (**G**) Prediction of the tertiary structure of calmodulin and calcineurin-A from Nile tilapia and mouse by SWISS-MODEL. (**H** and **I**) Phylogenetic trees for IP_3R (H) and calcineurin-A (I) were constructed with the amino acid sequences from the indicated species. The trees were constructed using the NJ algorithm in the Mega 4.1 program based on multiple sequence alignment by ClustalW. Bootstrap values of 1000 replicates (%) are indicated for the branches. The accession numbers of selected sequences are listed in Supplemental Table I.

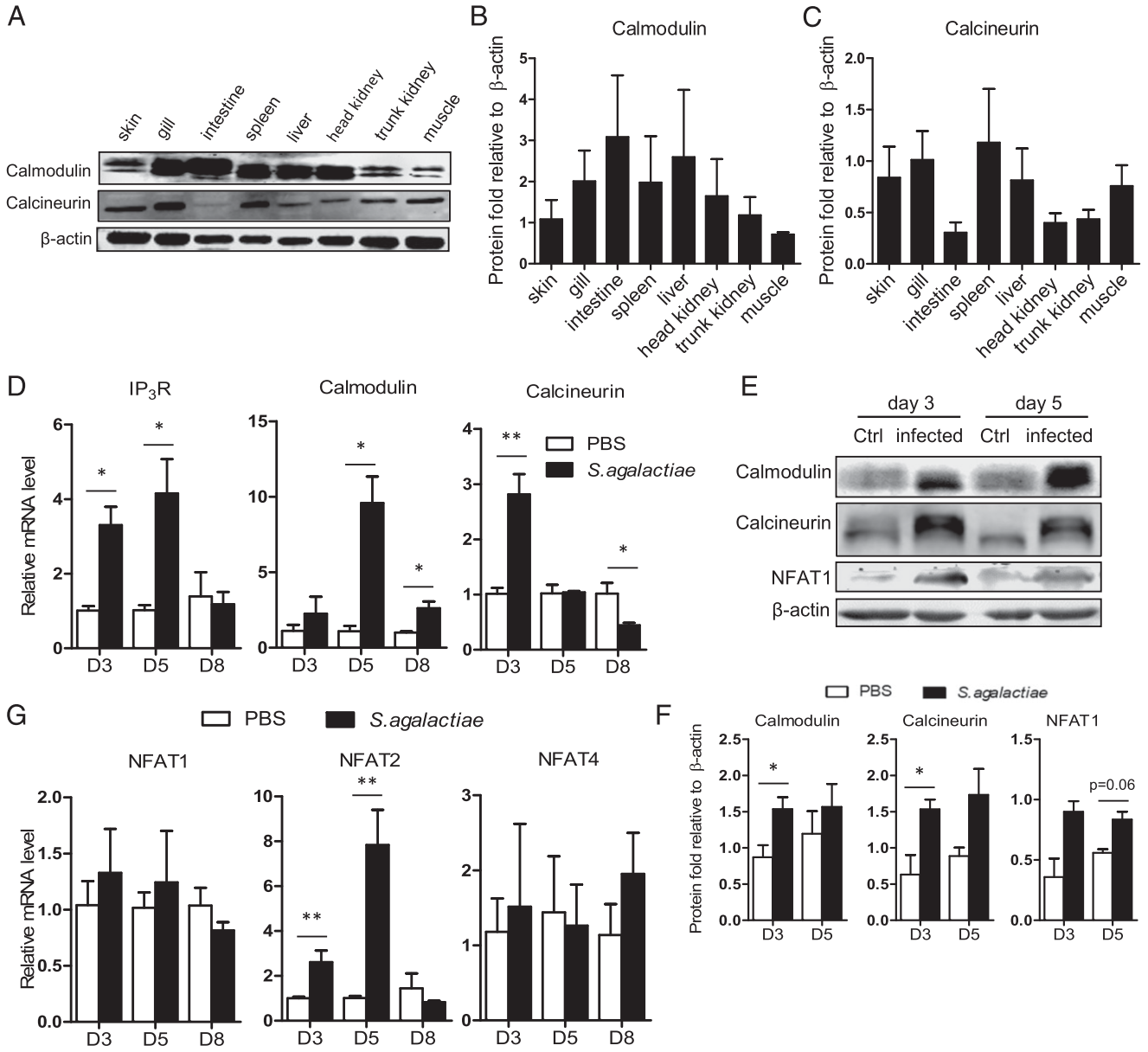

FIGURE 2. The Ca^{2+}–NFAT pathway is involved in the adaptive immune response of Nile tilapia. (**A**) Calmodulin and calcineurin-A expression in the indicated tissues was determined by Western blotting. (**B** and **C**) Quantification of calmodulin (B) and calcineurin (C) expression by calculating the densitometry of target protein/β-actin (n = 4). (**D**–**G**) Fish were i.p. injected with *S. agalactiae* or PBS, and spleen lymphocytes were harvested on the indicated days postinfection. (D and G) Relative mRNA levels of indicated molecules in lymphocytes with or without infection were examined by qPCR (n = 4–5). (E) Immunoblotting showed the expression pattern of the indicated molecules in lymphocytes with or without infection. (F) Quantification of indicated protein expression by calculating the densitometry of target protein/β-actin (n = 3). The data shown are representative of at least two independent experiments. $^*p < 0.05$, $^{**}p < 0.01$, as determined by a two-tailed Student t test.

phosphorylation rather than mRNA or protein level. Downstream of IP_3R, the mRNA level of calmodulin was significantly induced after lymphocytes were stimulated by PHA (Fig. 3A). Concordantly, we also found elevated protein expression of calmodulin in lymphocytes after activation by PMA plus ionomycin (Fig. 3B, 3D). Furthermore, although much weaker than thapsigargin-induced Ca^{2+} influx, an obvious and sustained Ca^{2+} influx accompanying PHA-induced T cell activation was observed by flow cytometry on the gated lymphocyte population (Fig. 3E, 3F). Although neither mRNA nor protein level of calcineurin was increased during T cell/lymphocyte activation (Fig. 3A, 3B), T cell or lymphocyte activation did cause a prompt increase in calcineurin enzyme activity (Fig. 3G, 3H). Altogether, our results suggest that IP_3R phosphorylation, calmodulin expression, sustained Ca^{2+} influx, and calcineurin activation are crucial events during Nile tilapia T cell activation.

Nile tilapia calcineurin-regulated NFAT nuclear import controls T cell activation

In mammals, TCR signal-induced Ca^{2+} influx and calcineurin activation are crucial for NFAT nuclear translocation and T cell activation. To determine whether these events is also indispensable for ancestral T cell activation, we first examined the expression and translocation patterns of NFAT upon T cell or lymphocyte activation. After PHA stimulation, mRNA expression of NFAT1, NFAT2, and NFAT4 in spleen lymphocytes was significantly upregulated (Fig. 4A), suggesting the potential involvement of NFAT in T cell activation at the transcriptional level. Total NFAT1 protein

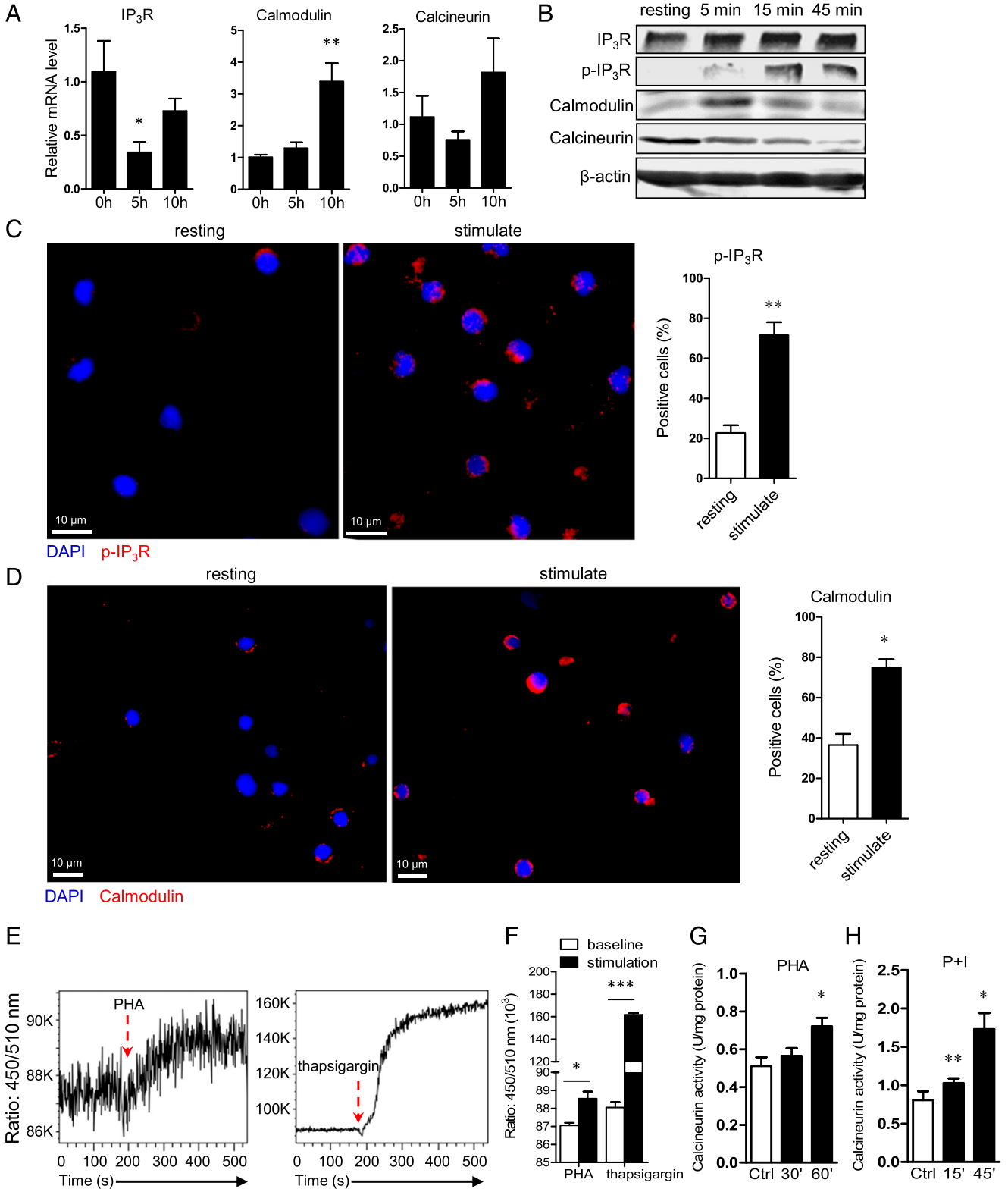

FIGURE 3. T cell signals induce Ca2+ influx and calcineurin activation in Nile tilapia. (**A**) Spleen lymphocytes of Nile tilapia were stimulated with PHA in vitro, and relative mRNA levels of the indicated molecules were examined by qPCR ($n = 4$). (**B–D**) Spleen lymphocytes were stimulated with PMA and ionomycin in vitro. (B) Immunoblotting showing protein or phosphoprotein levels of the indicated molecules in lymphocytes with or without stimulation. (C and D) Immunofluorescence analysis showing the level of IP_3R phosphorylation (C) and calmodulin (D) in lymphocytes with or without stimulation. Bar figures shown the percentage of positive cells within 100 cells ($n = 3$). (**E** and **F**) Ca^{2+} influx was determined by flow cytometry of Indo-1–loaded spleen lymphocytes based on the change in the 450:510 nm ratio after PHA or thapsigargin stimulation (E), and bar figure showing the ratio of 450:510 nm statistics before and after stimulation (F) ($n = 3$). (**G** and **H**) Enzyme activity of calcineurin was examined in Nile tilapia spleen lymphocytes after in vitro PHA (G) or PMA plus ionomycin (H) stimulation ($n = 3$). The data shown are representative of at least two independent experiments. $^*p < 0.05$, $^{**}p < 0.01$, $^{***}p < 0.001$, as determined by a two-tailed Student t test.

levels were also induced when spleen lymphocytes were activated by PMA plus ionomycin (Fig. 4B). More importantly, NFAT1 translocation into the nucleus increased notably within 15 min during this process (Fig. 4C). Elevated NFAT1 nuclear translocation upon lymphocyte activation was further confirmed by confocal microscopy (Fig. 4D). These results indicate that NFAT translocation is a remarkable event during lymphocyte activation in Nile tilapia.

To investigate the role of NFAT translocation on T cell activation in Nile tilapia, the calcineurin specific inhibitor cyclosporine A was employed to block Ca^{2+}–NFAT signaling. In vivo injection of cyclosporine A obviously suppressed the enzyme activity of calcineurin in Nile tilapia spleen lymphocytes after PHA stimulation (Fig. 4E) and further impaired nuclear translocation of NFAT1 (Fig. 4F). Moreover, blockade of calcineurin activity and NFAT translocation by cyclosporine A hindered upregulation of CD122 and IFN-γ during PHA-induced T cell activation (Fig. 4G, 4H), indicating that NFAT nuclear translocation is indispensable for T cell activation in Nile tilapia. Taken together, our results show that NFAT nuclear translocation induced by calcineurin activity plays a crucial role during T cell activation in the teleost Nile tilapia.

Cabin1 represses calcineurin activity to prevent NFAT-induced T cell activation

The activity of calcineurin is controlled not only by upstream Ca^{2+} and calmodulin, but also by several endogenous calcineurin inhibitors (10, 20). Among these inhibitors, the Cabin1 interacts with calcineurin to block its enzyme activity independently of calmodulin, resulting in inhibition of NFAT dephosphorylation and nuclear translocation (22, 23). A Cabin1 identified in the Nile tilapia genome displays the same domain organization as its homolog from human. In both proteins, the N terminus contains six tetratrico peptide repeat region (TPR) domains (Fig. 5A), which facilitate protein–protein interaction and multiprotein complex assembly, and the C terminus contains the MEF2-binding domain (Fig. 5A), whose interaction with MEF2 domain would cause repression of transcription (44). Compared with that of the human protein, amino acid sequence of the Nile tilapia protein, including but not limited to the MEF2-binding domain, is relatively conserved (Fig. 5B). In addition, the phylogenetic tree suggests that Nile tilapia Cabin1 clusters with homologs from other teleost (Fig. 5C). Therefore, Nile tilapia Cabin1 appears to be an evolutionarily conserved molecule that might perform similar functions with that in higher vertebrates.

Next, we assessed whether Nile tilapia Cabin1 influences calcineurin activity and NFAT nuclear import. Upon PHA-induced T cell activation, Cabin1 mRNA expression was notably increased in spleen lymphocytes from Nile tilapia (Fig. 5D). The efficient knockdown of Cabin1 expression by siRNA (Fig. 5E) significantly enhanced calcineurin enzyme activity (Fig. 5F), suggesting potential inhibition of calcineurin activity by Cabin1 in Nile tilapia. Furthermore, increased calcineurin activity induced by Cabin1 interference was accompanied by higher levels of NFAT1 protein in the nucleus of Nile tilapia spleen lymphocytes (Fig. 5G). Concordantly, spleen lymphocytes isolated from Cabin1–siRNA-treated fish exhibited a stronger T cell activation status, as manifested by obviously elevated CD122 and IFN-γ mRNA expression (Fig. 5H). Altogether, our data indicate that Cabin1 prevents NFAT-induced T cell activation of Nile tilapia by repressing calcineurin enzyme activity.

DYRK1A promotes NFAT nuclear export in Nile tilapia

In addition to the calcineurin-regulated NFAT nuclear import, NFAT-driven gene expression is controlled by several NFAT kinases in the nucleus, which promote NFAT rephosphorylation, nuclear export signal exposure and nuclear export (30, 31). We identified a homolog of NFAT kinase, DYRK1A, in the Nile tilapia genome. The amino acid sequence of Nile tilapia DYRK1A, especially the functional protein kinase domain, is highly conserved compared with the corresponding sequences from mouse (Fig. 6A). Moreover, DYRK1As from Nile tilapia and mouse share almost identical domain organization and tertiary structure (Fig. 6B, 6C), suggesting evolutionary conservation of this kinase. Similar to other molecules that regulate Ca^{2+}–NFAT signaling, Nile tilapia DYRK1A shows close evolutionary distance with teleost species (Fig. 6D). Based on these sequence, structure, and phylogenetic properties of Nile tilapia DYRK1A, we suspect that it performs a similar regulatory function in the context of NFAT nuclear translocation.

In Nile tilapia spleen lymphocytes, the mRNA expression of DYRK1A was dramatically increased following activation by PHA (Fig. 6E), suggesting its potential involvement in T cell activation. To investigate the regulatory role of DYRK1A in Nile tilapia NFAT nuclear translocation, we treated fish with the specific inhibitor harmine before spleen lymphocytes were stimulated with PMA and ionomycin. Inhibition of DYRK1A caused more NFAT1 protein to be retained in the nucleus during lymphocyte activation (Fig. 6F), indicating that DYRK1A promotes NFAT nuclear export. In accordance with the higher level of nuclear NFAT1, T cells from DYRK1A-inhibited fish were more easily activated than were those from normal animals, as revealed by the higher expression levels of CD122 and IFN-γ in response to PHA stimulation (Fig. 6G). Thus, DYRK1A-mediated NFAT nuclear export negatively regulates T cell activation in Nile tilapia. Meanwhile, we found that DYRK1A blockade by harmine enhanced GSK3β phosphorylation in spleen lymphocytes during PMA and ionomycin stimulation (Fig. 6H). GSK3 is another reported NFAT kinase that promotes NFAT nuclear export in mammals (10, 29), and both mRNA and phosphorylation levels of Nile tilapia GSK3 were enhanced during T cell activation (Fig. 6I, 6J). Because phosphorylation of GSK3 inactivates it, our results indicate that DYRK1A might regulate NFAT nuclear export via GSK3 in Nile tilapia.

Teleost NFAT might cooperate with other transcription factors to initiate gene expression

The NFAT protein has been considered to be an important factor for integrating of Ca^{2+} signaling with many other pathways in T cells, because it can interact with different transcription factors to initiate T cell–specific gene expression in the nucleus (10, 20). AP1, NIP-45, EGR-1, IRF-4, and T-bet are well-known mammalian transcription partners of NFAT, and their interactions with NFAT are crucial for IL-2, IL-4, or IFN-γ expression and T cell activation (45–50). Using coimmunoprecipitation assay, Nile tilapia NFAT1 was found to directly associate with the AP1 component c-Fos, NIP-45, T-bet, and IRF4 (Fig. 7A–D), suggesting the potential regulatory roles of NFAT in T cell gene expression. However, Nile tilapia NFAT1 could not associate with EGR-1 (Fig. 7E). We also revealed that Nile tilapia NFAT1 is able to form a homodimer (Fig. 7F). In contrast, depending on the milieu, NFAT interacts with Foxp3 at the IL-2 promoter to inhibit IL-2 expression and suppress T cell activation (51). Interestingly, the interaction between NFAT1 and Foxp3 is also observed in Nile tilapia (Fig. 7G), indicating its potential negative regulatory effect on T cell immunity. Altogether, these data suggest that teleost NFAT might serve as a versatile integrator that cooperates with multiple transcription factors to regulate T cell immunity.

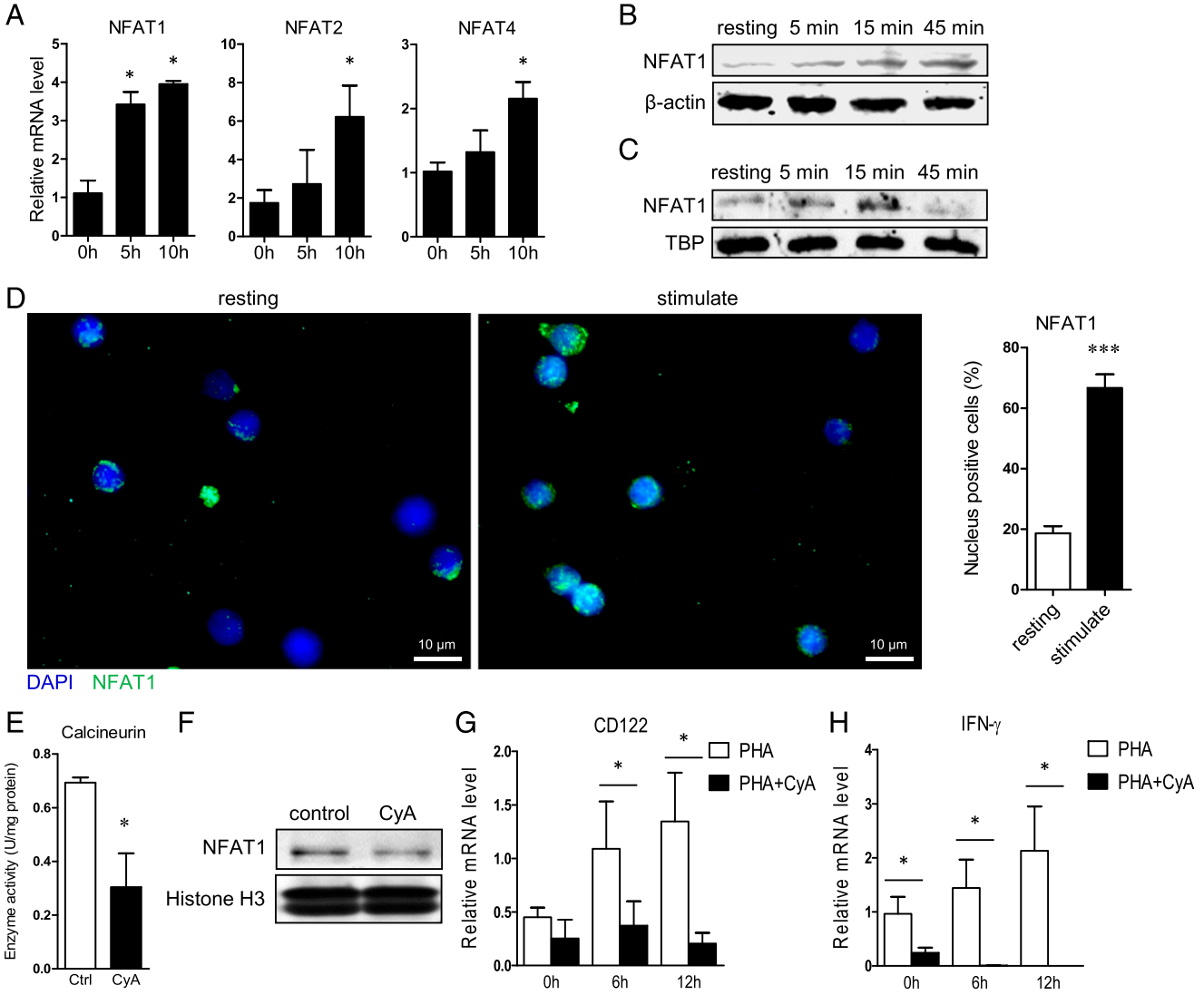

FIGURE 4. Calcineurin-regulated NFAT nuclear import is crucial for Nile tilapia T cell activation. (**A**) Spleen lymphocytes of Nile tilapia were stimulated with PHA in vitro, and relative mRNA levels of the indicated molecules were examined by qPCR ($n = 4$). (**B**–**D**) Spleen lymphocytes were stimulated with PMA and ionomycin in vitro. (B and C) Immunoblotting showing protein levels of NFAT1 among total protein (B) or nuclear protein (C) of lymphocytes with or without stimulation. (D) Immunofluorescence analysis showing NFAT1 levels in lymphocytes with or without stimulation. Bar figure shown the percentage of nucleus positive cells within 100 positive cells ($n = 3$). (**E**–**H**) Nile tilapia individuals were treated with cyclosporine A for two consecutive days, and lymphocytes were stimulated with PHA or PMA plus ionomycin in vitro. (E) Enzyme activity of calcineurin in cyclosporine A–treated or untreated spleen lymphocytes after PHA stimulation ($n = 3$). (F) Immunoblotting showing the protein level of NFAT1 in the nuclear protein fraction of cyclosporine A–treated or untreated lymphocytes after PMA plus ionomycin stimulation. (G and H) Bar figures show the relative mRNA levels of the indicated molecules in cyclosporine A–treated or untreated spleen lymphocytes after PHA stimulation ($n = 4$). The data shown are representative of two independent experiments. $^*p < 0.05$, $^{***}p < 0.001$, as determined by a two-tailed Student t test.

Teleost T cell requires Ca^{2+}–NFAT signaling for proper expansion during the antibacterial response

Upon activation, T cells rapidly proliferate and differentiate into effector T cells to eliminate infection. Because Ca^{2+}–NFAT signaling is crucial for Nile tilapia T cell activation, we sought to know whether this signaling controls T cell expansion during the primary immune response. Nile tilapia was treated with cyclosporine A during *S. agalactiae* infection. The relative spleen and head kidney weights of infected animals were obviously increased at 8 d postinfection (Fig. 8A). In contrast, the gaining weight of immune related organs was dramatically impaired in fish whose Ca^{2+}–NFAT signaling were blocked (Fig. 8A). Furthermore, the total leukocyte numbers isolated from spleen and head kidney of cyclosporine A–treated fish were markedly reduced compared with those from infected control animals (Fig. 8B). Our previous results revealed that cyclosporine A treatment decreases the frequencies of lymphocyte population in the PBL and spleen of Nile tilapia during *S. agalactiae* infection (42). In the current study, we found that inhibition of Ca^{2+}–NFAT signaling caused an obvious decrease of lymphocyte frequencies, not only in PBL and spleen, but also in the head kidney (Fig. 8C, 8D). The lower leukocyte numbers and lymphocyte frequencies in the spleen and head kidney in the absence of Ca^{2+}–NFAT activity collectively resulted in a severe reduction of lymphocyte numbers compared with those in infected control fish (Fig. 8E). These observations suggest that Ca^{2+}–NFAT signaling is indispensable for pathogen-induced lymphocyte expansion in teleost.

S. agalactiae infection induces mRNA expression of TCR and coreceptors in Nile tilapia lymphocytes (42). In our study, a dramatic decrease expression of TCRβ, CD4-1 and CD8α mRNA in spleen lymphocytes treated with cyclosporine A was observed on

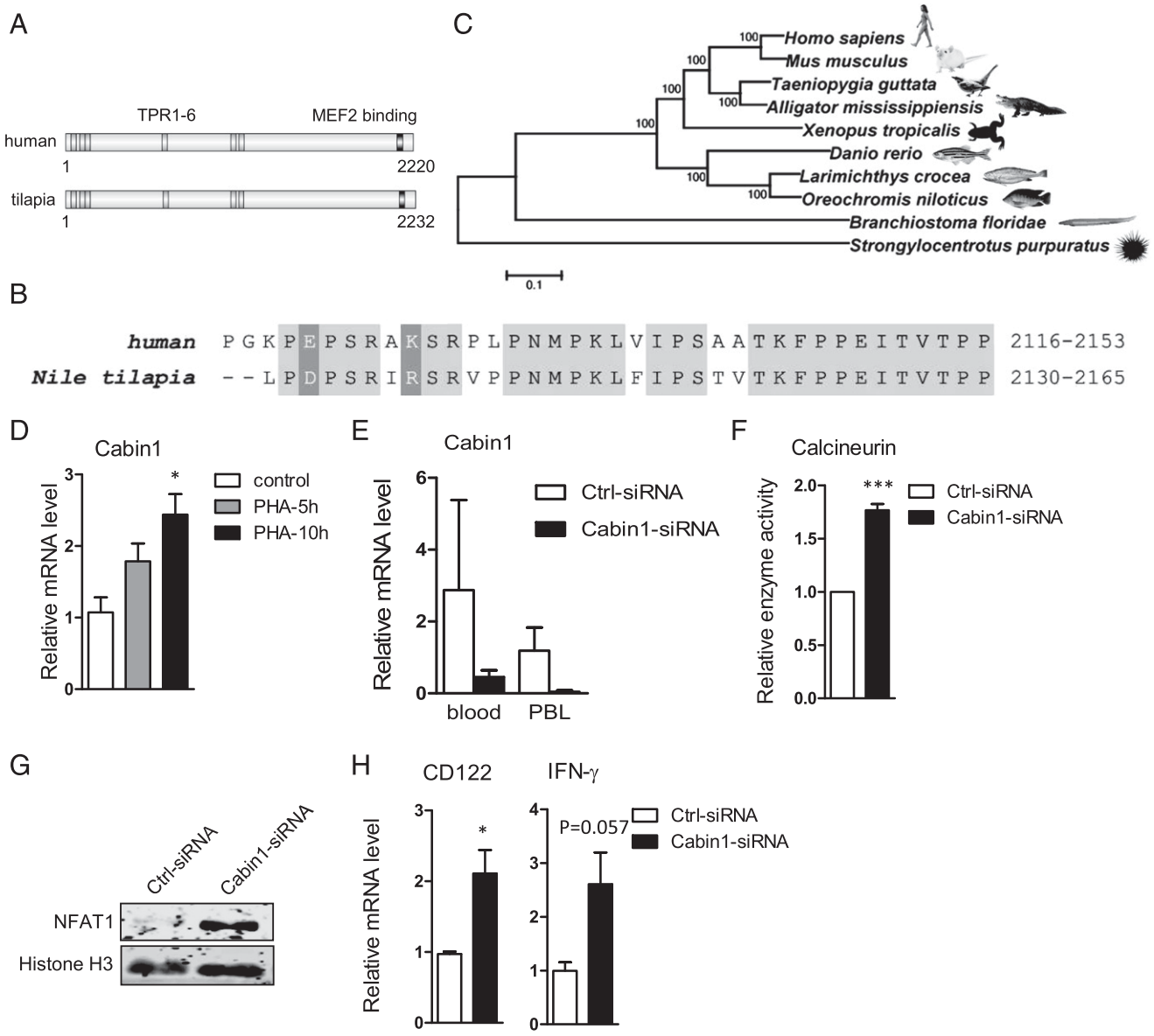

FIGURE 5. Cabin1 represses calcineurin and prevents NFAT nuclear import-driven T cell activation. (**A**) Comparison of the domain organization of Cabin1 from the indicated species. (**B**) Alignment analysis of the MEF2-binding domain of Nile tilapia Cabin1 with its homolog in human. Amino acid residues with 100% identity are in light gray, and similar amino acids are in dark gray. (**C**) A phylogenetic tree for Cabin1 was constructed with the amino acid sequences from the indicated species. The trees were constructed using the NJ algorithm with the Mega 4.1 program based on multiple sequence alignment by ClustalW. Bootstrap values of 1000 replicates (%) are indicated for the branches. The accession numbers of selected sequences are listed in Supplemental Table I. (**D**) Spleen lymphocytes of Nile tilapia were stimulated with PHA in vitro, and the relative mRNA level of Cabin1 was examined by qPCR (n = 4). (**E**–**H**) Nile tilapia was i.p. injected with control- or Cabin1-siRNA, and cells were harvested for assay at 48 h after injection. (E) Bar figure shows the relative mRNA level of Cabin1 in blood or PBL after injection of the indicated siRNA (n = 4). (F) Relative calcineurin enzyme activity in spleen lymphocytes injected with control- or Cabin1-siRNA (n = 4). (G) Immunoblotting showing NFAT1 levels in the nuclei of spleen lymphocytes from siRNA-injected fish. (H) Relative mRNA levels of the indicated molecules in spleen lymphocytes after siRNA injection (n = 4). The data shown are representative of two independent experiments. $*p < 0.05$, $***p < 0.001$, as determined by a two-tailed Student t test.

day 5 after *S. agalactiae* infection (Fig. 8F), suggesting the potential regulatory role of Ca^{2+}–NFAT signaling on proliferation of the T cell lineage in Nile tilapia. To investigate this regulation, CFSE-labeled Nile tilapia spleen lymphocytes were stimulated with PHA in the presence or absence of cyclosporine A. Upon PHA-induced T cell activation, a severely defective proliferation was detected in lymphocytes lacking of Ca^{2+}–NFAT activity (Fig. 8G). Meanwhile, inhibition of Ca^{2+}–NFAT signaling might not affect lymphocyte survival, because the frequencies of $7AAD^+$ cells were comparable between the Ca^{2+}–NFAT inhibited and uninhibited groups (Fig. 8G). To further confirm the regulatory effect of Ca^{2+}–NFAT signaling on the clonal expansion of the T cell lineage in vivo, an anti-LCK Ab, which could specifically identify Nile tilapia T cells (42), was used to trace T cells during *S. agalactiae* infection. Ca^{2+}–NFAT suppression by cyclosporine A resulted in a marked defect in T cell frequency, as indicated by LCK^+ cells among the gated spleen lymphocyte population (Fig. 8H, 8I). In addition to the frequency of LCK^+ cells, the level of LCK expression was decreased in cyclosporine A–treated spleen lymphocytes (Fig. 8J). Collectively, these observations suggest that Ca^{2+}–NFAT signaling promotes pathogen-induced expansion of T cells in Nile tilapia.

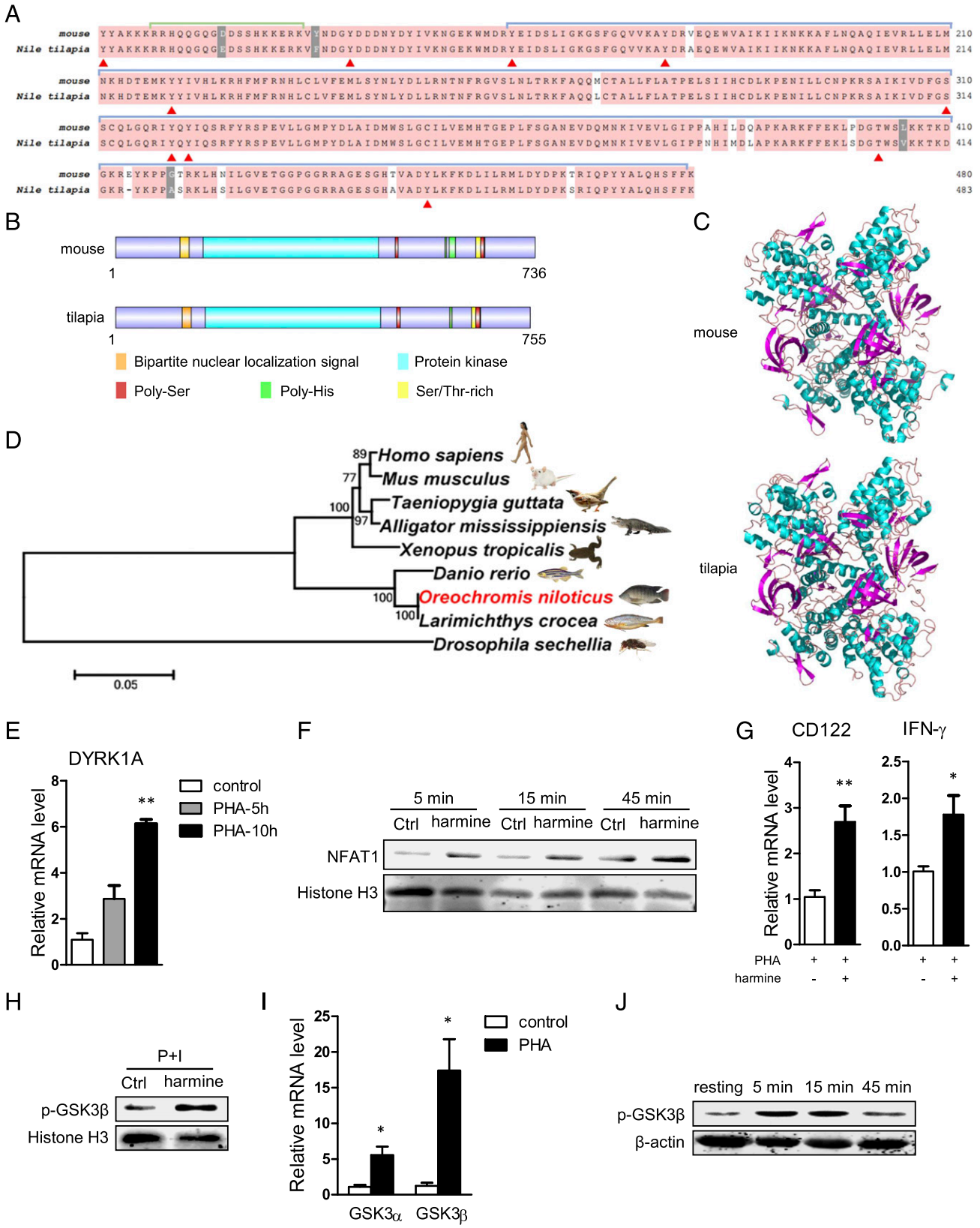

FIGURE 6. DYRK1A promotes NFAT nuclear export in Nile tilapia. (**A**) Alignment analysis of the functional domain of Nile tilapia DYRK1A with its homolog in mouse. Amino acid residues with 100% identity are in red, and similar amino acids are in gray. The bipartite nuclear localization signal is marked with a green line, the protein kinase domain is marked with a blue line, and the autophosphorylation sites are labeled with a red triangle. (**B**) Comparison of the domain organization of DYRK1A from the indicated species. (**C**) Prediction of the tertiary structure of DYRK1A from Nile tilapia and mouse by SWISS-MODEL. (**D**) A phylogenetic tree for DYRK1A was constructed with the amino acid sequences from the indicated species. The trees were constructed using the NJ algorithm with the Mega 4.1 program based on multiple sequence alignment by ClustalW. Bootstrap values of 1000 replicates (%) are indicated for the branches. The accession numbers of selected sequences are listed in Supplemental Table I. (**E**) Spleen lymphocytes of Nile tilapia were stimulated with PHA in vitro, and the relative mRNA level of DYRK1A was examined by qPCR *(Figure legend continues)*

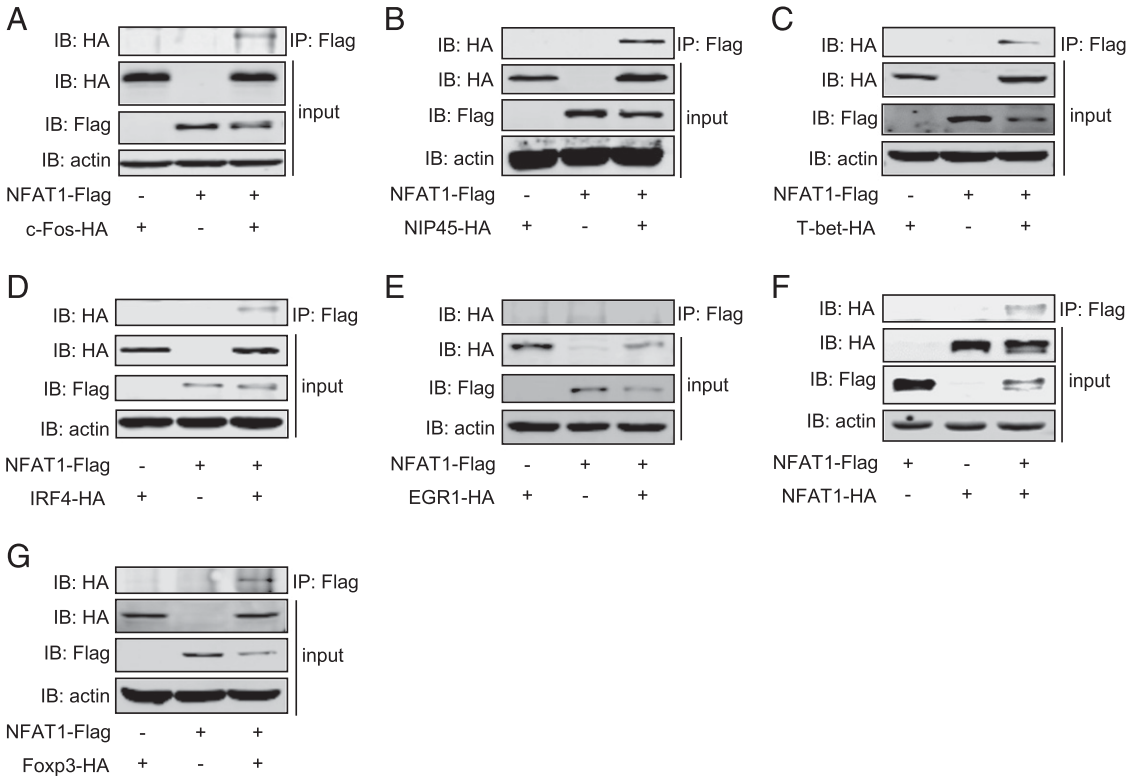

FIGURE 7. Interaction of Nile tilapia NFAT1 with its transcription factor partners. 293 T cells cotransfected with NFAT1-Flag-pEGFP-C1 and partner-HA-pEGFP-C1 were subjected to immunoblotting analysis directly for input control or after immunoprecipitation with anti-Flag Ab-conjugated agarose beads. Immunoblotting was performed using the indicated Abs. (**A**–**G**) Interaction of Nile tilapia NFAT1 with c-Fos (A), NIP-45 (B), T-bet (C), IRF4 (D), EGR1 (E), NFAT1 (F), or Foxp3 (G). The data shown are representative of two independent experiments.

Activity of Ca^{2+}–NFAT axis is indispensable for Nile tilapia T cells to eliminate infection

Because Ca^{2+}–NFAT signaling is pivotal for Nile tilapia T cell proliferation during the antibacterial immune response, we next sought to determine whether defective expansion of T cells affects their ability to eliminate infection. Blockade of Ca^{2+}–NFAT activity by cyclosporine A during *S. agalactiae* infection rendered the fish more vulnerable to pathogen (Fig. 9A). The high mortality rate of animals lacking of Ca^{2+}–NFAT activity was associated with a hampered ability to control the infection, as shown by dramatical higher bacterial burdens in both spleen and liver compared with the corresponding control (Fig. 9B). Recent studies have elucidated the indispensable roles of cytotoxic T cells or INF-γ-producing Th1 cells in controlling infection caused by extracellular *Streptococcus* pathogens in both mammals and teleost (42, 52, 53). We found that inhibition of Ca^{2+}–NFAT activity impaired expression of the cytotoxic-related gene perforin A, but not granzyme B, in spleen lymphocytes during *S. agalactiae* infection (Fig. 9C). Meanwhile, transcriptional levels of the proinflammatory cytokines IFN-γ and LT-α, as well as the proapoptotic gene FasL, were obviously lower in lymphocytes isolated from cyclosporine A–treated Nile tilapia than in those from control fish (Fig. 9D, 9E). Moreover, expression of T-bet, an effector $CD8^+$ T cell transcription factor, was also reduced in the absence of Ca^{2+}–NFAT activity (Fig. 9F). Therefore, the results suggest that activity of Ca^{2+}–NFAT axis is indispensable for Nile tilapia T cells to eliminate infection.

Altogether, in Nile tilapia, T cell signaling induces IP_3R phosphorylation, Ca^{2+} influx, and calcineurin activation, subsequently promoting NFAT nuclear import (Fig. 10A). In the nucleus, in conjunction with transcription factors from other signaling, NFAT initiates expression of genes that are responsible for T cell activation (Fig. 10A). In addition, Ca^{2+}–NFAT activity is indispensable for Nile tilapia T cell proliferation and infection elimination (Fig. 10B). Ca^{2+}–NFAT signaling-controlled T cell immunity is regulated at multiple levels in Nile tilapia, and exogenous cyclosporine A and endogenous Cabin1 suppress calcineurin-driven NFAT nuclear import, whereas DYRK1A promotes NFAT nuclear export (Fig. 10A).

Discussion

Ca^{2+} is a versatile second messenger that controls numerous cellular processes. Binding of Ca^{2+} to alter the charge of organelles and protein conformation represents a widespread and primitive signal transduction mechanism (32). Different cell types adopt

($n = 4$). (**F**–**H**) Nile tilapia individuals were treated with the DYRK1A inhibitor harmine for two consecutive days, and spleen lymphocytes were stimulated with PHA or PMA plus ionomycin in vitro. (F) Immunoblotting showed the protein level of NFAT1 in the nuclear protein fraction of harmine-treated or untreated lymphocytes after PMA plus ionomycin stimulation. (G) Bar figures show the relative mRNA levels of the indicated molecules in harmine-treated or untreated spleen lymphocytes after PHA stimulation ($n = 4$). (H) Immunoblotting demonstrated the phosphorylation level of GSK3β in the nuclear protein fraction of harmine-treated or untreated lymphocytes at 15 min after PMA plus ionomycin stimulation. (**I**) Spleen lymphocytes of Nile tilapia were stimulated with PHA in vitro, and the relative mRNA level of GSK3α or GSK3β was examined by qPCR ($n = 4$). (**J**) Immunoblotting indicating the phosphorylation level of GSK3β in spleen lymphocytes with or without PMA plus ionomycin stimulation. The data shown are representative of two independent experiments. $*p < 0.05$, $**p < 0.01$, as determined by a two-tailed Student t test.

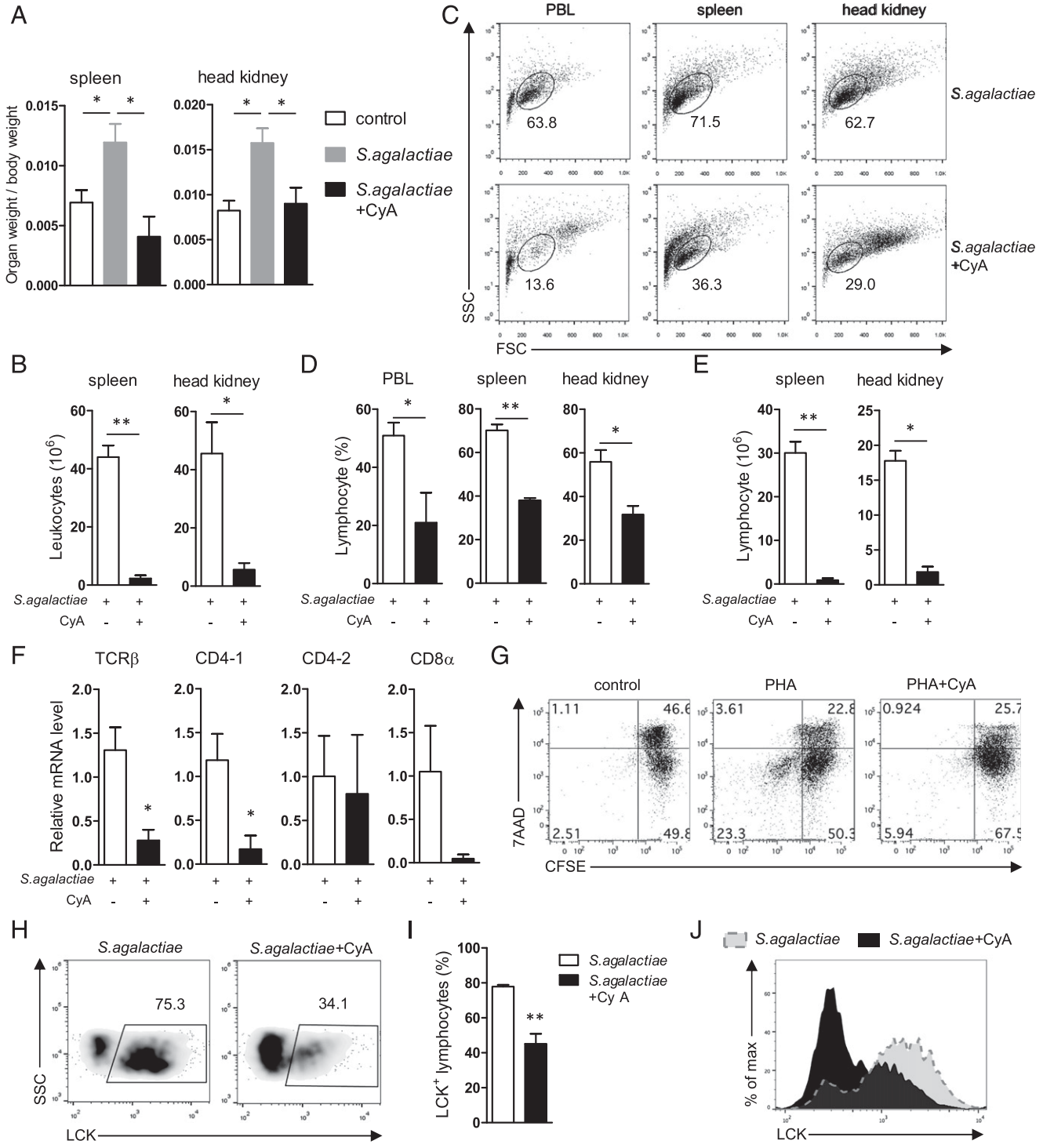

FIGURE 8. Ca^{2+}–NFAT signaling is indispensable for Nile tilapia T lymphocyte expansion during the antibacterial response. Nile tilapia individuals infected with *S. agalactiae* were i.p. injected with cyclosporine A on days 2, 3, 4, and 6, and the animals were sacrificed for assay on day 8. (**A** and **B**) Relative organ weight (A) and leukocyte number (B) of the spleen and head kidney of cyclosporine A–treated or untreated fish ($n = 4$). (**C**–**E**) Representative dot plots (C), percentage (D), and absolute number (E) of lymphocytes within PBL, spleen, and head kidney leukocytes ($n = 4$). (**F**) Nile tilapia infected with *S. agalactiae* were i.p. injected with cyclosporine A on days 2, 3, and 4, and relative mRNA expression of the indicated molecules in spleen lymphocytes was examined by qPCR on day 5 postinfection ($n = 4$–5). (**G**) Nile tilapia individuals were treated with cyclosporine A for two consecutive days, and spleen lymphocytes were labeled with CFSE and stimulated with PHA in the presence or absence of additional cyclosporine A. The dot plot shows the CFSE and 7AAD staining at 48 h after stimulation. (**H**–**J**) Nile tilapia individuals infected with *S. agalactiae* were i.p. injected with cyclosporine A on days 2, 3, 4, and 6, and the animals were sacrificed for assay on day 8. (H) Representative density plots showing the frequencies of LCK^+ lymphocytes in the spleen. (I) Bar figures show the percentage of LCK^+ lymphocytes in the spleen ($n = 4$). (J) Overlaid histograms showing LCK expression in spleen lymphocytes with or without cyclosporine A treatment. The data shown are representative of two independent experiments. $^*p < 0.05$, $^{**}p < 0.01$, as determined by a two-tailed Student *t* test.

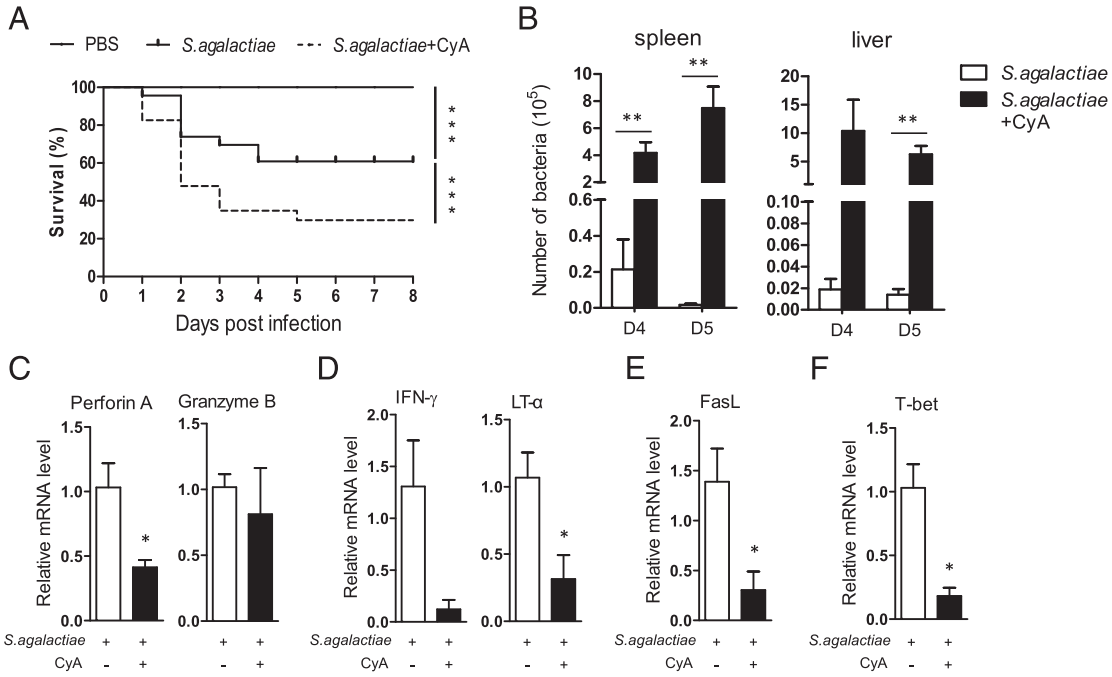

FIGURE 9. Ca^{2+}–NFAT signaling is critical for Nile tilapia effector cells to eliminate infection. Nile tilapia individuals infected with *S. agalactiae* were i.p. injected with cyclosporine A on days 2, 3, 4, and 6. (**A**) Kaplan–Meyer survival plot showing the survival percentage of Nile tilapia with or without cyclosporine A treatment postinfection ($n = 20$). $^{***}p < 0.001$. The data shown are representative of three independent experiments. (**B**) *S. agalactiae* titers in the spleen and liver on the indicated day postinfection ($n = 5$). (**C**–**F**) Relative mRNA levels of the indicated molecules in spleen lymphocytes with or without cyclosporine A treatment on day 8 after *S. agalactiae* infection ($n = 4$). The data shown are representative of two independent experiments. $^{*}p < 0.05$, $^{**}p < 0.01$, as determined by a two-tailed Student *t* test.

distinct sets of Ca^{2+} signaling molecules. As with other excitable cells, lymphocytes express ion channels to ensure Ca^{2+} influx/efflux as well as physiological functions, such as gene expression, development, migration, and apoptosis (3, 4, 15). During the past decade, essential regulatory roles of Ca^{2+} influx in T cell immune processes, including maturation, activation, proliferation, differentiation, and function, have been well elucidated in mammalian models (4, 5, 8–10, 14, 15). Nevertheless, whether and how Ca^{2+} signaling modulates the T cell response in early vertebrates remains unclear. In the current study, we found that tight regulation of calcineurin–NFAT axis activation by Ca^{2+} influx is indispensable for ancestral T cell activation, proliferation, and infection clearance in a fish species. Because regulatory mechanism of T cell immunity is not well understood in teleost, we anticipate the findings of this study will fill in an important gap in our knowledge regarding mechanism of adaptive immunity in early vertebrates and provide a valuable perspective on T cell evolution.

Bony fish has evolved an integral adaptive immune system armed with fundamental weapons similar to those of tetrapod, for example, B cells that express IgM/D/T, T cells with diverse subpopulations, and cytokines (IL-2, IL-4, IFN-γ, etc.) with specific regulatory functions (36, 54–56). Recent evidence demonstrates the paramount importance of teleost IgT^+ B cells in resisting parasite infection in mucosal sites (55, 57–59). In contrast, suspected T cell subpopulations, such as $CD4^+$, $CD8^+$, or $TCR\gamma\delta^+$ leukocytes, also exert immunological functions similar to those of helper T cells, cytotoxic T cells, or APCs in mammals (33–36, 38, 41). Despite great progress regarding teleost lymphocyte function, the underlying mechanisms by which these cells develop, activate, proliferate, or differentiate are largely unknown. For teleost T cells, the slow progress is largely due to the lack of effective mAbs of CD3ε for all T cells or TCRβ for αβ T cells. In our previous study, we found that a mAb against human LCK was able to identify the T cell population from Nile tilapia lymphocytes and revealed that mTORC1 signaling is indispensable for teleost T cell activation and effector function via controlling metabolic reprogramming (42). Using the Nile tilapia model, we further illustrate in this study the potential mechanism by which Ca^{2+}–NFAT signaling regulates teleost T cell activation and function. The lymphocyte signaling agonist PMA plus ionomycin, T cell–specific mitogen PHA, and anti-LCK Ab were used to exclude interference from other cell lineages. Meanwhile, to block Ca^{2+}–NFAT signaling in Nile tilapia, an immunosuppressive agent that is widely used in organ transplantation, cyclosporine A, was employed. Although such inhibition cannot exclude effects from other cell lineages, our study provides valuable evidence for understanding the regulatory mechanism of ancestral T cells. Knockout model based on LCK or CD4 Cre-driven CRISPR/Cas9 is expected to facilitate further elucidation of the intrinsic regulatory roles of Ca^{2+}–NFAT signaling in teleost T cell immunity.

Recent comparative genomic studies focusing on Ca^{2+} signaling have suggested that animals, fungi, and plants use different mechanisms to control cytosolic Ca^{2+} concentrations, indicating that Ca^{2+} signaling acquired more extensive and varied functions when life evolved from prokaryotic organisms to multicellular eukaryotes (32). However, whether Ca^{2+} signaling and its regulation on physiological processes, such as T cell immunity, evolved within vertebrates remains unknown. The bony fish Nile tilapia encodes the highly conserved components of Ca^{2+}–calcineurin–NFAT axis, and these molecules were found to be distributed widely in tissues/organs, suggesting potential versatile functions of teleost Ca^{2+} signaling, as reported in mammals. Ca^{2+}–calcineurin-driven NFAT activation is of paramount importance for T cell activation. In mammals, TCR engagement results in the phosphorylation of PLCγ1, which further hydrolyzes PIP2 to generate the second messenger IP_3; IP_3 in turn binds to its receptor on the ER membrane to trigger intracellular Ca^{2+} depletion and

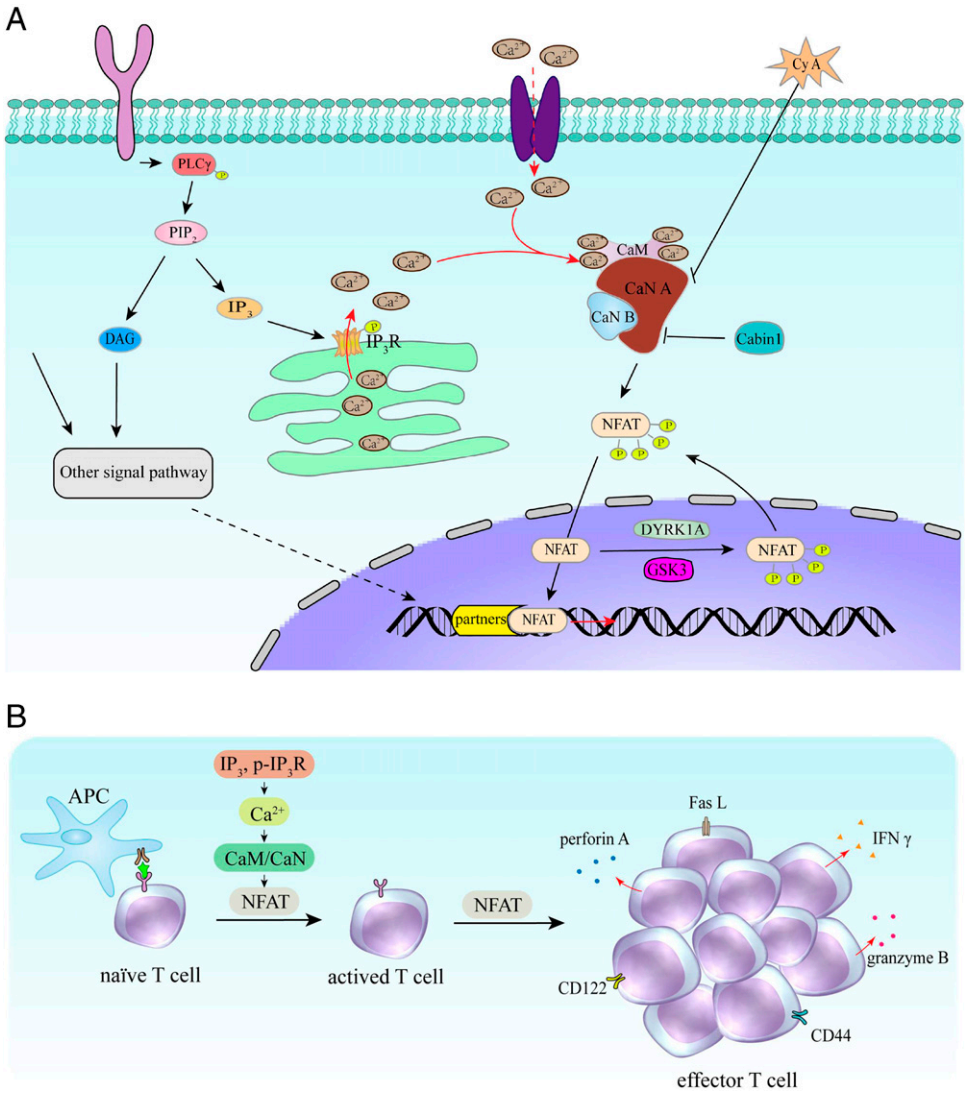

FIGURE 10. Ca^{2+}–calcineurin signaling-controlled NFAT translocation is crucial for proper activation and function of fish T cells. (**A**) In Nile tilapia, T cell signals induce IP_3R phosphorylation, sustained Ca^{2+} influx, calmodulin (CaM) elevation, and calcineurin (CaN) activation, subsequently promoting NFAT nuclear import. In the nuclear, NFAT associates with transcription factors from other signaling pathways and initiates transcription of genes that are responsible for T cell activation. Ca^{2+}–NFAT signaling-controlled T cell activation is regulated by exogenous cyclosporine A and endogenous Cabin1, which suppress calcineurin-driven NFAT nuclear import, as well as by nuclear DYRK1A, which promotes NFAT nuclear export. (**B**) Ca^{2+}–NFAT signaling plays significant roles in Nile tilapia T cell activation, proliferation and effector T cell–mediated infection clearance.

sustained Ca^{2+} influx (4, 9). Binding to Ca^{2+} alters the conformation of calmodulin and activates calcineurin to promote gene transcription driven by nuclear import of NFAT, and this transcription is indispensable for T cell activation and function (5, 8). Strikingly, by examining Nile tilapia, we found that these events of the Ca^{2+}–NFAT regulatory strategy are not specific for modern T cells; instead, they had already emerged in primitive T cells of teleost during their activation. Moreover, Nile tilapia T cells employ Cabin1 to suppress calcineurin activity, and DYRK1A to promote NFAT nuclear export, which are also sophisticated strategies for modern T cells (10, 20). Thus, our data support an argument that Ca^{2+}–NFAT-modulated T cell activation might be an ancestral trait that already existed with the appearance of adaptive immunity prior to the divergence of bony fish from the tetrapod lineage. Downstream of calmodulin, the cAMP-responsive element-binding (CREB) protein, which is regulated by Ca^{2+}–calmodulin-dependent kinase (CaMK), also plays a central role in T cell–related gene transcription after T cell activation (8). Further study is needed to elucidate the potential cooperative roles of Ca^{2+}–calmodulin–CaMK–CREB axis in teleost T cell immunity.

To a large extent, the functional versatility of Ca^{2+}–NFAT signaling in T cell immunity can be attributed to the ability of this axis to integrate signals from other pathways (10, 20). AP1, a dimer that is formed by c-Fos and c-Jun that downstream of MAPK signaling, is the best characterized transcriptional partner of NFAT, and its cooperation with NFAT is responsible for a specific pattern of gene expression that is essential for T cell activation (46, 50). Nevertheless, AP1 is not the only transcriptional partner of NFAT that synergistically influences gene expression. For example, NFAT binds with c-Maf, IRF-4, or NIP-45 at the IL-4 promoter to favor its expression (45, 49, 60); NFAT also cooperates with EGR-1 or IRF-4 to activate the IL-2 promoter (48, 61, 62). In addition, NFAT and STAT4 together induce IFN-γ expression and work synergistically with the transcription factor T-bet to maintain Th1 cells and commit cells to Th1 differentiation (10, 20, 47). In Treg cells, NFAT directs T cell tolerance via formation of the NFAT:Foxp3:DNA complex, which displaces the

NFAT:AP1:DNA complex, to suppress IL-2 expression (51). Structurally, flexibility of the linker region between N- and C-terminal regions of RHD is responsible for the broad binding ability of NFAT with other transcription factors (10). The high conservation of Nile tilapia NFAT1 with its homologs from mammals indicates that this protein may have similar synergistic roles with its partners in teleost. As expected, Nile tilapia NFAT1 was found to specifically associate with c-Fos, NIP-45, T-bet, IRF4, and Foxp3 in our present study. In addition to interaction with other transcription factors, Nile tilapia NFAT1 forms a homodimer, which is expected to occupy palindromic sites in gene regulatory regions and to turn on specific gene-expression programs (63, 64). Although the exact gene expression driven by the interaction of NFAT with its transcription partners needs to be further elucidated in Nile tilapia, our preliminary data provide helpful evidence for understanding the potential regulatory mechanism of Ca^{2+}–NFAT signaling in T cell immunity in a fish species.

Ca^{2+}–NFAT signaling is crucially important for adaptive immune response that confers resistance to pathogen infection. Mammals with deficiencies in intracellular Ca^{2+} depletion, Ca^{2+} influx, calcineurin activity, or NFAT nuclear import show severe defects in T cell immunity (4, 5, 15–17) and are even at high risk of SCID, which is associated with uncontrollable bacterial infection and high mortality (18, 19). In our study, we found that expression of Nile tilapia Ca^{2+}–NFAT signaling components was obviously induced by bacterial infection; moreover, suppression of signaling activity by cyclosporine A impaired T cell activation, expansion, and infection clearance, rendering the animals more vulnerable to pathogens. These observations suggest that, as in modern mammals, Ca^{2+}–NFAT signaling-regulated T cell immunity is a key strategy for resisting invasion of pathogenic microorganisms in early vertebrates. However, many immunological events, including but not limited to the regulation of Ca^{2+} channels, the relationships among different NFATs, and the intrinsic roles of Ca^{2+}–NFAT signaling in T cell immunity, should be elucidated in the future.

In summary, after identifying an evolutionarily conserved Ca^{2+}–NFAT pathway in Nile tilapia, we elucidated its activation mechanisms in a fish species. More importantly, we found that Ca^{2+}–NFAT signaling is indispensable for the activation, proliferation, and infection clearance of primordial T cells in jawed fish, thus providing the first description, to our knowledge, regarding regulatory roles of Ca^{2+}–NFAT signaling-mediated T cell immunity in a nontetrapod. Mechanistically, our data obtained using this early vertebrate revealed interaction of NFAT with several other transcription factors and clarified the potential regulatory mechanisms of NFAT nuclear translocation. Because knowledge of adaptive immunity in early vertebrates remains limited, our results have shed light on the mechanism of T cell immunity in teleost. Moreover, from an evolutionary perspective, we propose that Ca^{2+}–NFAT-modulated T cell immunity is a primitive strategy that already existed upon the appearance of ancestral T cells, prior to the divergence of bony fish from the tetrapod lineage.

Acknowledgments

We thank Dr. Pin Nie (Qingdao Agricultural University) for kindly providing the pEGFP-C1 plasmid and Dr. Baojun Zhang (Xi'an Jiaotong University) for kindly providing the HEK 293T cell line. We thank the Instruments Sharing Platform of the School of Life Sciences of ECNU for instruments sharing, the Flow Cytometry Core Facility of the School of Life Sciences of ECNU for the FACS analysis, and the ECNU Multifunctional Platform for Innovation (011) for animal keeping.

Disclosures

The authors have no financial conflicts of interest.

References

1. Clapham, D. E. 2007. Calcium signaling. *Cell* 131: 1047–1058.
2. Berridge, M. J., P. Lipp, and M. D. Bootman. 2000. The versatility and universality of calcium signalling. *Nat. Rev. Mol. Cell Biol.* 1: 11–21.
3. Feske, S., J. Giltnane, R. Dolmetsch, L. M. Staudt, and A. Rao. 2001. Gene regulation mediated by calcium signals in T lymphocytes. [Published erratum appears in 2008 *Nat Immunol*. 9: 328–329] *Nat. Immunol.* 9: 316–324.
4. Trebak, M., and J. P. Kinet. 2019. Calcium signalling in T cells. *Nat. Rev. Immunol.* 19: 154–169.
5. Feske, S., H. Wulff, and E. Y. Skolnik. 2015. Ion channels in innate and adaptive immunity. *Annu. Rev. Immunol.* 33: 291–353.
6. Koretzky, G. A., and P. S. Myung. 2001. Positive and negative regulation of T-cell activation by adaptor proteins. *Nat. Rev. Immunol.* 1: 95–107.
7. Smith-Garvin, J. E., G. A. Koretzky, and M. S. Jordan. 2009. T cell activation. *Annu. Rev. Immunol.* 27: 591–619.
8. Oh-hora, M. 2009. Calcium signaling in the development and function of T-lineage cells. *Immunol. Rev.* 231: 210–224.
9. Quintana, A., D. Griesemer, E. C. Schwarz, and M. Hoth. 2005. Calcium-dependent activation of T-lymphocytes. *Pflugers Arch.* 450: 1–12.
10. Macian, F. 2005. NFAT proteins: key regulators of T-cell development and function. *Nat. Rev. Immunol.* 5: 472–484.
11. Baine, I., B. T. Abe, and F. Macian. 2009. Regulation of T-cell tolerance by calcium/NFAT signaling. *Immunol. Rev.* 231: 225–240.
12. Müller, M. R., and A. Rao. 2010. NFAT, immunity and cancer: a transcription factor comes of age. *Nat. Rev. Immunol.* 10: 645–656.
13. Oh-hora, M., and A. Rao. 2009. The calcium/NFAT pathway: role in development and function of regulatory T cells. *Microbes Infect.* 11: 612–619.
14. Vaeth, M., M. Maus, S. Klein-Hessling, E. Freinkman, J. Yang, M. Eckstein, S. Cameron, S. E. Turvey, E. Serfling, F. Berberich-Siebelt, et al. 2017. Store-operated Ca^{2+} entry controls clonal expansion of T cells through metabolic reprogramming. *Immunity* 47: 664–679.e6.
15. Feske, S., E. Y. Skolnik, and M. Prakriya. 2012. Ion channels and transporters in lymphocyte function and immunity. *Nat. Rev. Immunol.* 12: 532–547.
16. Kaufmann, U., P. J. Shaw, L. Kozhaya, R. Subramanian, K. Gaida, D. Unutmaz, H. J. McBride, and S. Feske. 2016. Selective ORAI1 inhibition ameliorates autoimmune central nervous system inflammation by suppressing effector but not regulatory T cell function. *J. Immunol.* 196: 573–585.
17. Kim, K. D., S. Srikanth, Y. V. Tan, M. K. Yee, M. Jew, R. Damoiseaux, M. E. Jung, S. Shimizu, D. S. An, B. Ribalet, et al. 2014. Calcium signaling via Orai1 is essential for induction of the nuclear orphan receptor pathway to drive Th17 differentiation. *J. Immunol.* 192: 110–122.
18. Le Deist, F., C. Hivroz, M. Partiseti, C. Thomas, H. A. Buc, M. Oleastro, B. Belohradsky, D. Choquet, and A. Fischer. 1995. A primary T-cell immunodeficiency associated with defective transmembrane calcium influx. *Blood* 85: 1053–1062.
19. Feske, S., J. M. Müller, D. Graf, R. A. Kroczek, R. Dräger, C. Niemeyer, P. A. Baeuerle, H. H. Peter, and M. Schlesier. 1996. Severe combined immunodeficiency due to defective binding of the nuclear factor of activated T cells in T lymphocytes of two male siblings. *Eur. J. Immunol.* 26: 2119–2126.
20. Savignac, M., B. Mellström, and J. R. Naranjo. 2007. Calcium-dependent transcription of cytokine genes in T lymphocytes. *Pflugers Arch.* 454: 523–533.
21. Rothermel, B., R. B. Vega, J. Yang, H. Wu, R. Bassel-Duby, and R. S. Williams. 2000. A protein encoded within the Down syndrome critical region is enriched in striated muscles and inhibits calcineurin signaling. *J. Biol. Chem.* 275: 8719–8725.
22. Lai, M. M., P. E. Burnett, H. Wolosker, S. Blackshaw, and S. H. Snyder. 1998. Cain, a novel physiologic protein inhibitor of calcineurin. *J. Biol. Chem.* 273: 18325–18331.
23. Sun, L., H. D. Youn, C. Loh, M. Stolow, W. He, and J. O. Liu. 1998. Cabin 1, a negative regulator for calcineurin signaling in T lymphocytes. *Immunity* 8: 703–711.
24. Kashishian, A., M. Howard, C. Loh, W. M. Gallatin, M. F. Hoekstra, and Y. Lai. 1998. AKAP79 inhibits calcineurin through a site distinct from the immunophilin-binding region. *J. Biol. Chem.* 273: 27412–27419.
25. Klauck, T. M., M. C. Faux, K. Labudda, L. K. Langeberg, S. Jaken, and J. D. Scott. 1996. Coordination of three signaling enzymes by AKAP79, a mammalian scaffold protein. *Science* 271: 1589–1592.
26. Ryeom, S., R. J. Greenwald, A. H. Sharpe, and F. McKeon. 2003. The threshold pattern of calcineurin-dependent gene expression is altered by loss of the endogenous inhibitor calcipressin. *Nat. Immunol.* 4: 874–881.
27. Esau, C., M. Boes, H. D. Youn, L. Tatterson, J. O. Liu, and J. Chen. 2001. Deletion of calcineurin and myocyte enhancer factor 2 (MEF2) binding domain of Cabin1 results in enhanced cytokine gene expression in T cells. *J. Exp. Med.* 194: 1449–1459.
28. Zhu, J., F. Shibasaki, R. Price, J. C. Guillemot, T. Yano, V. Dötsch, G. Wagner, P. Ferrara, and F. McKeon. 1998. Intramolecular masking of nuclear import signal on NF-AT4 by casein kinase I and MEKK1. *Cell* 93: 851–861.
29. Beals, C. R., C. M. Sheridan, C. W. Turck, P. Gardner, and G. R. Crabtree. 1997. Nuclear export of NF-ATc enhanced by glycogen synthase kinase-3. *Science* 275: 1930–1934.
30. Gwack, Y., S. Sharma, J. Nardone, B. Tanasa, A. Iuga, S. Srikanth, H. Okamura, D. Bolton, S. Feske, P. G. Hogan, and A. Rao. 2006. A genome-wide Drosophila RNAi screen identifies DYRK-family kinases as regulators of NFAT. *Nature* 441: 646–650.
31. Arron, J. R., M. M. Winslow, A. Polleri, C. P. Chang, H. Wu, X. Gao, J. R. Neilson, L. Chen, J. J. Heit, S. K. Kim, et al. 2006. NFAT dysregulation by increased dosage of DSCR1 and DYRK1A on chromosome 21. *Nature* 441: 595–600.

32. Cai, X., X. Wang, S. Patel, and D. E. Clapham. 2015. Insights into the early evolution of animal calcium signaling machinery: a unicellular point of view. *Cell Calcium* 57: 166–173.
33. Araki, K., K. Akatsu, H. Suetake, K. Kikuchi, and Y. Suzuki. 2008. Characterization of CD8+ leukocytes in fugu (Takifugu rubripes) with antiserum against fugu CD8alpha. *Dev. Comp. Immunol.* 32: 850–858.
34. Wan, F., C. B. Hu, J. X. Ma, K. Gao, L. X. Xiang, and J. Z. Shao. 2017. Characterization of γδ T cells from zebrafish provides insights into their important role in adaptive humoral immunity. *Front. Immunol.* 7: 675.
35. Takizawa, F., S. Magadan, D. Parra, Z. Xu, T. Korytář, P. Boudinot, and J. O. Sunyer. 2016. Novel teleost CD4-bearing cell populations provide insights into the evolutionary origins and primordial roles of CD4+ lymphocytes and CD4+ macrophages. *J. Immunol.* 196: 4522–4535.
36. Nakanishi, T., Y. Shibasaki, and Y. Matsuura. 2015. T cells in fish. *Biology (Basel)* 4: 640–663.
37. Nakanishi, T., U. Fischer, J. M. Dijkstra, S. Hasegawa, T. Somamoto, N. Okamoto, and M. Ototake. 2002. Cytotoxic T cell function in fish. *Dev. Comp. Immunol.* 26: 131–139.
38. Takizawa, F., J. M. Dijkstra, P. Kotterba, T. Korytář, H. Kock, B. Köllner, B. Jaureguiberry, T. Nakanishi, and U. Fischer. 2011. The expression of CD8α discriminates distinct T cell subsets in teleost fish. *Dev. Comp. Immunol.* 35: 752–763.
39. Wen, Y., W. Fang, L. X. Xiang, R. L. Pan, and J. Z. Shao. 2011. Identification of Treg-like cells in Tetraodon: insight into the origin of regulatory T subsets during early vertebrate evolution. *Cell. Mol. Life Sci.* 68: 2615–2626.
40. Hui, S. P., D. Z. Sheng, K. Sugimoto, A. Gonzalez-Rajal, S. Nakagawa, D. Hesselson, and K. Kikuchi. 2017. Zebrafish regulatory T cells mediate organ-specific regenerative programs. *Dev. Cell* 43: 659–672.e5.
41. Zhu, L. Y., P. P. Pan, W. Fang, J. Z. Shao, and L. X. Xiang. 2012. Essential role of IL-4 and IL-4Rα interaction in adaptive immunity of zebrafish: insight into the origin of Th2-like regulatory mechanism in ancient vertebrates. *J. Immunol.* 188: 5571–5584.
42. Wei, X., K. Ai, H. Li, Y. Zhang, K. Li, and J. Yang. 2019. Ancestral T cells in fish require mTORC1-coupled immune signals and metabolic programming for proper activation and function. *J. Immunol.* 203: 1172–1188.
43. Brawand, D., C. E. Wagner, Y. I. Li, M. Malinsky, I. Keller, S. Fan, O. Simakov, A. Y. Ng, Z. W. Lim, E. Bezault, et al. 2014. The genomic substrate for adaptive radiation in African cichlid fish. *Nature* 513: 375–381.
44. Han, A., F. Pan, J. C. Stroud, H. D. Youn, J. O. Liu, and L. Chen. 2003. Sequence-specific recruitment of transcriptional co-repressor Cabin1 by myocyte enhancer factor-2. *Nature* 422: 730–734.
45. Rengarajan, J., K. A. Mowen, K. D. McBride, E. D. Smith, H. Singh, and L. H. Glimcher. 2002. Interferon regulatory factor 4 (IRF4) interacts with NFATc2 to modulate interleukin 4 gene expression. *J. Exp. Med.* 195: 1003–1012.
46. Macián, F., C. López-Rodríguez, and A. Rao. 2001. Partners in transcription: NFAT and AP-1. *Oncogene* 20: 2476–2489.
47. Lee, D. U., O. Avni, L. Chen, and A. Rao. 2004. A distal enhancer in the interferon-gamma (IFN-gamma) locus revealed by genome sequence comparison. *J. Biol. Chem.* 279: 4802–4810.
48. Hu, C. M., S. Y. Jang, J. C. Fanzo, and A. B. Pernis. 2002. Modulation of T cell cytokine production by interferon regulatory factor-4. *J. Biol. Chem.* 277: 49238–49246.
49. Hodge, M. R., H. J. Chun, J. Rengarajan, A. Alt, R. Lieberson, and L. H. Glimcher. 1996. NF-AT-Driven interleukin-4 transcription potentiated by NIP45. *Science* 274: 1903–1905.
50. Chen, L., J. N. M. Glover, P. G. Hogan, A. Rao, and S. C. Harrison. 1998. Structure of the DNA-binding domains from NFAT, Fos and Jun bound specifically to DNA. *Nature* 392: 42–48.
51. Wu, Y., M. Borde, V. Heissmeyer, M. Feuerer, A. D. Lapan, J. C. Stroud, D. L. Bates, L. Guo, A. Han, S. F. Ziegler, et al. 2006. FOXP3 controls regulatory T cell function through cooperation with NFAT. *Cell* 126: 375–387.
52. Weber, S. E., H. Tian, and L. A. Pirofski. 2011. CD8+ cells enhance resistance to pulmonary serotype 3 Streptococcus pneumoniae infection in mice. *J. Immunol.* 186: 432–442.
53. Olliver, M., J. Hiew, P. Mellroth, B. Henriques-Normark, and P. Bergman. 2011. Human monocytes promote Th1 and Th17 responses to *Streptococcus pneumoniae*. *Infect. Immun.* 79: 4210–4217.
54. Li, J., D. R. Barreda, Y. A. Zhang, H. Boshra, A. E. Gelman, S. Lapatra, L. Tort, and J. O. Sunyer. 2006. B lymphocytes from early vertebrates have potent phagocytic and microbicidal abilities. *Nat. Immunol.* 7: 1116–1124.
55. Zhang, Y. A., I. Salinas, J. Li, D. Parra, S. Bjork, Z. Xu, S. E. LaPatra, J. Bartholomew, and J. O. Sunyer. 2010. IgT, a primitive immunoglobulin class specialized in mucosal immunity. *Nat. Immunol.* 11: 827–835.
56. Zou, J., and C. J. Secombes. 2016. The function of fish cytokines. *Biology (Basel)* 5: E23.
57. Yu, Y. Y., W. Kong, Y. X. Yin, F. Dong, Z. Y. Huang, G. M. Yin, S. Dong, I. Salinas, Y. A. Zhang, and Z. Xu. 2018. Mucosal immunoglobulins protect the olfactory organ of teleost fish against parasitic infection. *PLoS Pathog.* 14: e1007251.
58. Xu, Z., F. Takizawa, D. Parra, D. Gómez, L. von Gersdorff Jørgensen, S. E. LaPatra, and J. O. Sunyer. 2016. Mucosal immunoglobulins at respiratory surfaces mark an ancient association that predates the emergence of tetrapods. *Nat. Commun.* 7: 10728.
59. Xu, Z., D. Parra, D. Gómez, I. Salinas, Y. A. Zhang, L. von Gersdorff Jørgensen, R. D. Heinecke, K. Buchmann, S. LaPatra, and J. O. Sunyer. 2013. Teleost skin, an ancient mucosal surface that elicits gut-like immune responses. *Proc. Natl. Acad. Sci. USA* 110: 13097–13102.
60. Ho, I. C., M. R. Hodge, J. W. Rooney, and L. H. Glimcher. 1996. The proto-oncogene c-maf is responsible for tissue-specific expression of interleukin-4. *Cell* 85: 973–983.
61. Decker, E. L., C. Skerka, and P. F. Zipfel. 1998. The early growth response protein (EGR-1) regulates interleukin-2 transcription by synergistic interaction with the nuclear factor of activated T cells. *J. Biol. Chem.* 273: 26923–26930.
62. Decker, E. L., N. Nehmann, E. Kampen, H. Eibel, P. F. Zipfel, and C. Skerka. 2003. Early growth response proteins (EGR) and nuclear factors of activated T cells (NFAT) form heterodimers and regulate proinflammatory cytokine gene expression. *Nucleic Acids Res.* 31: 911–921.
63. Jin, L., P. Sliz, L. Chen, F. Macián, A. Rao, P. G. Hogan, and S. C. Harrison. 2003. An asymmetric NFAT1 dimer on a pseudo-palindromic kappa B-like DNA site. *Nat. Struct. Biol.* 10: 807–811.
64. Giffin, M. J., J. C. Stroud, D. L. Bates, K. D. von Koenig, J. Hardin, and L. Chen. 2003. Structure of NFAT1 bound as a dimer to the HIV-1 LTR kappa B element. *Nat. Struct. Biol.* 10: 800–806.